We thank both reviewers for their comments.
Replies and changes are listed below.

# 1 General presentation

Following both reviewers' comments, the manuscript has been revised extensively. Most significantly,

1. The usage of acronyms has been greatly reduced in the text, in order to improve readability. In figures, we have chosen to replace SDRECS by the more compact $DRE^{sw}_{clr}$.

2. The conclusions have been revised to better emphasize, the results that may be model specific from those that are applicable to others models participating in CMIP6.

# 2 Reviewer 1

1. **the paper effectively does not consider the role of fires in their model / data comparisons. Consequently, the comparisons between data and model over India Asia (in particular) and anywhere in the tropics will be substantively compromised (e.g. Ramanathan and Carmichael, Nat Geo 2008 and references therein). In fact it seems likely that their poor model/data comparison in the tropics is likely because fires are not obviously considered in the comparison.**
Our model includes monthly biomass burning emissions from Global Fire Emissions Database. We agree with the reviewer that uncertainties in biomass burning could contribute to model biases in tropical regions. However, decadal changes in biomass burning are small relative to those in anthropogenic emissions in the regions that we focus on (India, China, the Eastern US, and Europe), which suggests it is unlikely to contribute to errors in the simulated trends in the aerosol effect. We have have added a reference to the van der Werf et al. [2017], which describes the methodology used to derived GFED emissions and highlighted that it is based on satellite observations. See also reply to comment 5 and to comment 4 from reviewer 2.
The text was revised as follow:

   *Monthly biomass burning emissions are from the historical global biomass burning emissions inventory for CMIP6 (BB4CMIP6, van Marle et al. [2017]). Emissions for the 1997 to 2015 period in this inventory have been derived from satellite-based emissions from the Global Fire Emissions Database (GFED, van der Werf et al. [2017]).*

2. **Line 165: What does this mean? this is apparently one of the many "p-tests" that gets used about the literature but essentially has no meaning if not explained.**
We have revised the text as follow:

   *We use the non-parametric Mann-Kendall test [Kendall, 1938] to identify significant changes in the aerosol effect. This test quantifies monotonic correlations between two variables. It is based on a rank procedure that makes it less susceptible to outliers than the Pearson correlation and thus especially well-suited for the analysis of environmental dataset. Here, we use a critical p value of 0.05 for trend significance. When a significant trend is detected, we estimate the linear trend using the Theil-Sen method [Theil, 1950, Sen, 1968].*

3. **Line 216: (fix this statement) "Changes in AOD are dominated by spring and summer"**
We have revised the text as follow:

   *Observations show that the AOD decreases most in spring and summer*

4. **Line 231: ??? Again too much acronyms / jargon. What is conclusion about these differences?**
We have revised the text as follow:

   *In both Europe and the US, we find that the change in the aerosol effect inferred from the SYN calculation is larger than that estimated from CERES-EBAF outgoing radiation corrected for surface albedo changes (*$EBAF_C$ *and* $EBAF_M$*). The magnitude of the changes in the MATCH AOD, which is used to calculate the SYN estimate, is also greater than in more recent retrieval of AOD from MODIS (Table 1). This suggests that the rate of change in SYN aerosol effect may be biased high in Europe and Western Europe.*

5. **Line 353. . . no biomass burning as part of anthropogenic emissions? The bulk of fires is due to human activities so this is an odd statement. Perhaps you mean the subset that is not human driven? That said, you would see substantial differences between observed and actual outgoing radiation if you leave this term out (which you apparently do over the tropics).**
We have performed an additional simulation to estimate the forcing from biomass burning. The text was revised as follow:

*We estimate the forcing from biomass burning and non-biomass burning sources separately, as the contribution of anthropogenic activities to changes in biomass burning emissions remains uncertain [Heald et al., 2014]. The average 2001–2015 simulated direct radiative forcing from fires is -0.011* $\mathrm{W\,m^{-2}}$*, which falls within the range of previous model assessments (*$0.0 \pm 0.05 \mathrm{W\,m^{-2}}$*, [Myhre et al., 2013]).*

## 2.1 Reviewer 2

1. **Readability: A good illustration is the term SDRECS. While it is well defined in the paper, it is technical and not standard in similar literature. Why not simply write "change in outgoing radiation"? Most of the paper deals with shortwave under clear sky conditions, so this is implicit even from the title. The same goes for Rsutcsaf , Rsutcs and similar.**
The manuscript has been modified significantly to improve readability. Following both reviewers' recommendations most acronyms from the main text have been removed. There is no widely accepted acronym to designate the clear-sky shortwave direct aerosol effect. In figures, we have replaced SDRECS by $\mathrm{DRE}^{\mathrm{sw}}_{\mathrm{clr}}$, which we think is easier to understand. We have kept rsutcsaf and rsutcs notations as they are based on *CMIP6* naming convention (http://clipc-services.ceda.ac.uk/dreq/index/CMORvar.html). This is now clearly stated.

2. **One challenge, especially in the latter part of the paper (the regional trends and RF discussions), is to follow where the conclusions depend on the specific aerosol parametrizations of the GFDL model, and where they can be assumed to be more general. I would encourage the authors to add some further discussion of how model dependent the conclusions are. E.g. in the Conclusions, how general are the remarks about possible issues with the CEDS inventory? This is an important discussion for a dataset that will form the basis for much of CMIP6. A specific example: The authors conclude that "we find significant uncertainties in the CMIP6 emissions, including in the seasonality of NH3". In the paper, as far as I can understand, this is documented through the following: "We conducted a sensitivity simulation using the seasonality of NH3 column from AIRS (Warner et al., 2017) 265 to modulate NH3 emissions. We find that this revised seasonality significantly reduces the simulated winter trend in SDRECS (0.08 Wm — 2 dec — 1 ), improving the agreement with observations." I would expect some more discussion and documentation on this point, to make such a broad conclusion.**

   (a) We have added a figure in the supplementary materials comparing the seasonality of ammonia emissions modulated using CMIP6 seasonality and AIRS seasonality (see Fig. 1 below).

   (b) We have revised the conclusion to emphasize that some of the biases may be model specific while others are associated with CMIP6 emissions and will thus affect all models. The text was revised as follow:

   *Some of these biases may be model-specific, including the treatment of the mixing between sulfate and black carbon or the representation of the photochemistry of sulfate and nitrate. Others are attributed to the CMIP6 emissions and will likely affect other models. In particular, we find that the model bias in winter over India can be largely accounted for by uncertainties in the seasonality of ammonia and black carbon emissions. Similarly, comparisons between the CMIP6 and MEIC emission inventories over China suggest that the model bias in this region can be largely attributed to an underestimate of the reduction of* $\mathrm{SO_2}$ *emissions after 2007.*

3. **For the DRF discussion, it would be good to put the results in a broader context. AeroCom is mentioned; where is AM3 relative to the model mean in terms of forcing strengths? E.g. a comparison to the similar (but much less detailed) results in Myhre et al 2017, ACP ( https://www.atmos-chem-phys.net/17/2709/2017/) would be useful.**
We have added a comparison with the results from Myhre et al. [2017] in the RF section:

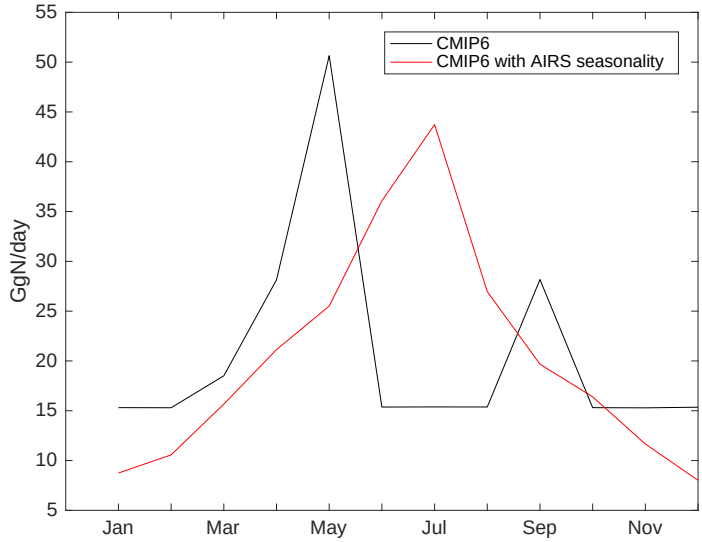


Figure 1: CMIP6 ammonia emissions for India with seasonality from CMIP6 (black) and AIRS (red)

*From 2001 to 2015, the direct aerosol forcing is simulated to be +0.03* $\mathrm{W\,m^{-2}}$*, including +0.12, -0.03, and -0.03* $\mathrm{W\,m^{-2}}$ *from black carbon, sulfate, and nitrate, respectively. Myhre et al. [2017] recently reported a similar change in the overall direct radiative forcing (+0.01* $\mathrm{W\,m^{-2}}$*) but different contributions from sulfate (+0.03* $\mathrm{W\,m^{-2}}$*) and black carbon (+0.03* $\mathrm{W\,m^{-2}}$*). Many factors could contribute to these differences including the radiative properties of aerosols (e.g., the mixing of sulfate with black carbon [Bond et al., 2013]) and the emission inventories. Further studies are needed to examine whether changes in the sensitivity of radiative forcing to anthropogenic emissions are robust across models. Such assessment would be especially important in the northern midlatitudes, where the direct radiative forcing from aerosols and greenhouse gases from 2001 to 2015 are simulated to be of similar magnitude (+0.25* $\mathrm{W\,m^{-2}}$*).*

4. **A more technical example: In Figure 1, introduced on line 177, the authors show both CEDS and MEIC emissions. However, "MEIC" isn't defined or discussed until line 300, making it difficult to understand even the first figure without already having read the entire manuscript. Please review for clarity, with a community reader in mind**
   We have added the following text in the method section
   *Anthropogenic emissions in India and China are expecte d to be more uncertain than in the US and Europe [Saikawa et al., 2017a,b]. Fig. 1 shows that the regional Modular Emission Inventory for China (MEIC) [Zhang et al., 2009], shows a decline of* $SO_2$ *emissions starting in 2006 and accelerating in 2012, a decrease of NO after 2012, and near-stable BC emissions after 2007. In 2014, MEIC NO,* $SO_2$*, and BC emissions are 24%, 48%, and 32% lower than CMIP6 emissions, respectively.* $NH_3$ *emissions are similar in magnitude but exhibit different seasonality: CMIP6* $NH_3$ *emissions peak in spring, while MEIC exhibits a broad peak in summer, consistent with top-down constraints [Paulot et al., 2014, Zhang et al., 2017].*

# References

T. C. Bond, S. J. Doherty, D. W. Fahey, P. M. Forster, T. Berntsen, B. J. DeAngelo, M. G. Flanner, S. Ghan, B. Kärcher, D. Koch, S. Kinne, Y. Kondo, P. K. Quinn, M. C. Sarofim, M. G. Schultz, M. Schulz, C. Venkataraman, H. Zhang, S. Zhang, N. Bellouin, S. K. Guttikunda, P. K. Hopke, M. Z. Jacobson, J. W. Kaiser, Z. Klimont, U. Lohmann, J. P. Schwarz, D. Shindell, T. Storelvmo, S. G. Warren, and C. S. Zender. Bounding the role of black carbon in the climate system: A scientific assessment. *Journal of Geophysical Research: Atmospheres*, 118(11): 5380–5552, 2013. ISSN 2169-8996. doi: 10.1002/jgrd.50171. URL `http://dx.doi.org/10.1002/jgrd.50171`.

C. L. Heald, D. A. Ridley, J. H. Kroll, S. R. H. Barrett, K. E. Cady-Pereira, M. J. Alvarado, and C. D. Holmes. Contrasting the direct radiative effect and direct radiative forcing of aerosols. *Atmos.*

*Chem. Phys.*, 14(11):5513–5527, June 2014. ISSN 1680-7324. doi: 10.5194/acp-14-5513-2014. URL http://www.atmos-chem-phys.net/14/5513/2014/.

M. G. Kendall. A new measure of rank correlation. *Biometrika*, 30(1-2):81–93, 1938. doi: 10.1093/biomet/30.1-2.81. URL + http://dx.doi.org/10.1093/biomet/30.1-2.81.

G. Myhre, B. H. Samset, M. Schulz, Y. Balkanski, S. Bauer, T. K. Berntsen, H. Bian, N. Bellouin, M. Chin, T. Diehl, R. C. Easter, J. Feichter, S. J. Ghan, D. Hauglustaine, T. Iversen, S. Kinne, A. Kirkevåg, J.-F. Lamarque, G. Lin, X. Liu, M. T. Lund, G. Luo, X. Ma, T. van Noije, J. E. Penner, P. J. Rasch, A. Ruiz, Ø. Seland, R. B. Skeie, P. Stier, T. Takemura, K. Tsigaridis, P. Wang, Z. Wang, L. Xu, H. Yu, F. Yu, J.-H. Yoon, K. Zhang, H. Zhang, and C. Zhou. Radiative forcing of the direct aerosol effect from AeroCom phase II simulations. *Atmos. Chem. Phys.*, 13(4):1853–1877, February 2013. ISSN 1680-7324.

G. Myhre, W. Aas, R. Cherian, W. Collins, G. Faluvegi, M. Flanner, P. Forster, Ø. Hodnebrog, Z. Klimont, M. T. Lund, J. Mülmenstädt, C. Lund Myhre, D. Olivié, M. Prather, J. Quaas, B. H. Samset, J. L. Schnell, M. Schulz, D. Shindell, R. B. Skeie, T. Takemura, and S. Tsyro. Multi-model simulations of aerosol and ozone radiative forcing due to anthropogenic emission changes during the period 1990–2015. *Atmospheric Chemistry and Physics*, 17(4): 2709–2720, 2017. doi: 10.5194/acp-17-2709-2017. URL https://www.atmos-chem-phys.net/17/2709/2017/.

F. Paulot, D. J. Jacob, R. W. Pinder, J. O. Bash, K. Travis, and D. K. Henze. Ammonia emissions in the United States, European Union, and China derived by high-resolution inversion of ammonium wet deposition data: Interpretation with a new agricultural emissions inventory (MASAGE_NH3). *J. Geophys. Res. Atmos.*, 119(7): 4343–4364, April 2014. ISSN 2169-8996.

Eri Saikawa, Hankyul Kim, Min Zhong, Alexander Avramov, Yu Zhao, Greet Janssens-Maenhout, Jun ichi Kurokawa, Zbigniew Klimont, Fabian Wagner, Vaishali Naik, Larry W. Horowitz, and Qiang Zhang. Comparison of emissions inventories of anthropogenic air pollutants and greenhouse gases in china. *Atmospheric Chemistry and Physics*, 17(10):6393–6421, may 2017a. doi: 10.5194/acp-17-6393-2017. URL https://doi.org/10.5194/acp-17-6393-2017.

Eri Saikawa, Marcus Trail, Min Zhong, Qianru Wu, Cindy L Young, Greet Janssens-Maenhout, Zbigniew Klimont, Fabian Wagner, Jun ichi Kurokawa, Ajay Singh Nagpure, and Bhola Ram Gurjar. Uncertainties in emissions estimates of greenhouse gases and air pollutants in india and their impacts on regional air quality. *Environmental Research Letters*, 12(6):065002, may 2017b. doi: 10.1088/1748-9326/aa6cb4. URL https://doi.org/10.1088/1748-9326/aa6cb4.

Pranab Kumar Sen. Estimates of the Regression Coefficient Based on Kendall's Tau. *J. Am. Stat. Assoc.*, 63(324):1379–1389, December 1968. ISSN 0162-1459. doi: 10.1080/01621459.1968.10480934. URL http://www.tandfonline.com/doi/abs/10.1080/01621459.1968.10480934.

H. Theil. A rank-invariant method of linear and polynomial regression analysis. I. *Nederl. Akad. Wetensch., Proc.*, 53:386–392 = Indagationes Math. 12, 85–91 (1950), 1950. URL http://www.ams.org/mathscinet-getitem?mr=0036489.

G. R. van der Werf, J. T. Randerson, L. Giglio, T. T. van Leeuwen, Y. Chen, B. M. Roğers, M. Mu, M. J. E. van Marle, D. C. Morton, G. J. Collatz, R. J. Yokelson, and P. S. K̃asibhatla. Global fire emissions estimates during 1997–2016. *Earth System Science Data*, 9(2):697–720, 2017. doi: 10.5194/essd-9-697-2017. URL https://www.earth-syst-sci-data.net/9/697/2017/.

Margreet J. E. van Marle, Silvia Kloster, Brian I. Magi, Jennifer R. Marlon, Anne-Laure Daniau, Robert D. Field, Almut Arneth, Matthew Forrest, Stijn Hantson, Natalie M. Kehrwald, Wolfgang Knorr, Gitta Lasslop, Fang Li, Stéphane Mangeon, Chao Yue, Johannes W. Kaiser, and Guido R. van der Werf. Historic global biomass burning emissions for CMIP6 (BB4cmip) based on merging satellite observations with proxies and fire models (1750–2015). *Geosci. Model Dev.*, 10(9):3329–3357, sep 2017. doi: 10.5194/gmd-10-3329-2017. URL https://doi.org/10.5194/gmd-10-3329-2017.

L. Zhang, Y. Chen, Y. Zhao, D. K. Henze, L. Zhu, Y. Song, F. Paulot, X. Liu, Y. Pan, and B. Huang. Agricultural ammonia emissions in China: reconciling bottom-up and top-down estimates. *Atmos. Chem. Phys. Discuss.*, 2017:1–36, August 2017. ISSN 1680-7375. doi: 10.5194/acp-2017-749. URL https://www.atmos-chem-phys-discuss.net/acp-2017-749/.

Q. Zhang, D. G. Streets, G. R. Carmichael, K. B. He, H. Huo, A. Kannari, Z. Klimont, I. S. Park, S. Reddy, J. S. Fu, D. Chen, L. Duan, Y. Lei, L. T. Wang, and Z. L. Yao. Asian emissions in 2006 for the NASA INTEX-B mission. *Atmos. Chem. Phys.*, 9(14):5131–5153, July 2009. ISSN 1680-7324. doi: 10.5194/acp-9-5131-2009. URL `https://www.atmos-chem-phys.net/9/5131/2009/`.

Manuscript prepared for Atmos. Chem. Phys.
with version 2014/09/16 7.15 Copernicus papers of the LaTeX class copernicus.cls.
Date: 21 May 2018

# Changes in the aerosol direct radiative forcing from 2001 to 2015: observational constraints and regional mechanisms

Fabien Paulot[1,2], David Paynter[1], Paul Ginoux[1], Vaishali Naik[1], and Larry W. Horowitz[1]

[1]Geophysical Fluid Dynamics Laboratory, National Oceanic and Atmospheric Administration, Princeton, New Jersey, USA
[2]Program in Atmospheric and Oceanic Sciences, Princeton University, New Jersey, USA

*Correspondence to:* Fabien.Paulot@noaa.gov

**Abstract.** We present ~~observation~~ observation- and model-based estimates of ~~the~~ changes in the ~~direct shortwave effect of aerosols under clear-sky (SDRECS)from 2001 to 2015.~~ aerosol direct clear-sky shortwave radiative effect ($DRE^{sw}_{clr}$), the perturbation by aerosols of the net downward shortwave clear-sky radiation at the top of the atmosphere. Observation-based estimates ~~are obtained from changes in~~ of $DRE^{sw}_{clr}$ are derived from the outgoing shortwave clear-sky radiation ~~(Rsutcs)~~ measured by the Clouds and the Earth's Radiant Energy System (CERES) ~~,~~accounting for the effect of variability in surface albedo, water vapor, and ozone. ~~We find increases in SDRECS~~ From 2001 to 2015, we find that $DRE^{sw}_{clr}$ increases (i.e., less radiation is scattered to space by aerosols) over Western Europe (0.7 – 1 $\mathrm{W\,m^{-2}\,dec^{-1}}$) and the Eastern US (0.9 – 1.8 $\mathrm{W\,m^{-2}\,dec^{-1}}$), decreases over India (-0.5 – -1.9 $\mathrm{W\,m^{-2}\,dec^{-1}}$)~~and no significant change~~ , and does not change significantly over Eastern China. ~~Comparisons with the GFDL chemistry climate~~ We show that the GFDL chemistry-climate model AM3, driven by CMIP6 historical emissions, ~~show that changes in SDRECS~~ captures changes over Western Europe (0.6 $\mathrm{W\,m^{-2}\,dec^{-1}}$) and the Eastern US ~~are wellcaptured, which largely~~ (0.8 $\mathrm{W\,m^{-2}\,dec^{-1}}$) well. This agreement reflects the mature understanding of the sulfate budget in these regions. In contrast, the model overestimates the ~~trends in SDRECS~~ change in $DRE^{sw}_{clr}$ over India and Eastern China. Over China, this bias can be partly attributed to the decline of $SO_2$ emissions after 2007, which is not captured ~~by~~ in the CMIP6 ~~emissions. In~~ emission inventory. Over India, the lack of change in the outgoing clear-sky shortwave radiation in the model is attributed to the compensation between the decreases of dust and surface albedo and the increase of anthropogenic aerosols. For both India and Eastern China, ~~we find much larger contributions of~~ model simulations indicate that nitrate and black carbon contribute more to changes

in ~~SDRECS~~ $DRE^{sw}_{clr}$ than in the US and Europe, which highlights the need to better constrain their ~~precursors~~ sources and chemistry. Globally, our model shows that changes in the all-sky aerosol direct ~~forcing~~ radiative forcing, the anthropogenic component of the aerosol direct radiative effect, between 2001 and 2015 (+0.03 $\mathrm{W\,m^{-2}}$) are dominated by black carbon (+0.12 $\mathrm{W\,m^{-2}}$) with significant offsets from nitrate (-0.03 $\mathrm{W\,m^{-2}}$) and sulfate (-0.03 $\mathrm{W\,m^{-2}}$). ~~Changes in the sulfate (+7%) and nitrate (+60%) all-sky direct forcing~~ AM3 also shows that changes in the speciation and spatial distribution of emissions between 2001 and 2015 ~~are only weakly related to changes in the emissions of their precursors (-12.5% and 19% for~~ have reduced the sensitivity of the aersosol direct radiative forcing to $SO_2$ ~~and $NH_3$, respectively), due mostly to chemical non linearities.~~ emissions (via sulfate aerosols), but increased that to ammonia and NO emissions (via nitrate aerosols).

## 1 Introduction

Aerosols affect climate (Boucher et al., 2013) both directly, via scattering and absorption of ~~incoming and outgoing~~ solar and terrestrial radiation (Charlson et al., 1992), and indirectly, by modulating the abundance of cloud condensation nuclei, the droplet size distribution, and the lifetime of clouds (Twomey, 1974; Rosenfeld et al., 2014). Storelvmo et al. (2016) estimated that the increase in the burden of atmospheric aerosols associated with anthropogenic activities has masked approximately ~~one third~~ one-third of the continental warming from greenhouse gases from 1964 to 2010, with important implications for global and regional climate (Wild, 2009; Bollasina et al., 2011). ~~In this work, we focus on the aerosol direct forcing.~~

~~Multi-model comparisons suggest that the direct aerosol forcing~~Previous studies have leveraged global spaceborne observations of the Earth's radiative budget (Wielicki et al., 1996, 1998) and aerosol abundance (Kahn et al., 2005; Levy et al., 2013b) to estimate the overall aerosol direct radiative effect (DRE), i.e., the direct perturbation of the Earth's radiative budget by ~~anthropogenic aerosols , was -0.27 $\mathrm{W\,m^{-2}}$ in~~ aerosols (Christopher and Zhang, 2004; Patadia et al., 2008; Loeb and Manalo-Smith, 2005; Kahn, 2012). Observational constraints for the aerosol direct radiative forcing (DRF), the anthropogenic component of the aerosol direct radiative effect, are less robust (Su et al., 2013; Bellouin et al., 2005, 2008), which contributes to the large spread in model estimates for DRF in 2000 relative to 1850 ~~(Myhre et al., 2013). However the large spread among models (-0.016~~ (-0.02 – -0.58 $\mathrm{W\,m^{-2}}$ ~~), complicates the assessment of the climate impact of anthropogenic aerosols. Previous studies have leveraged global spaceborne observations of the Earth Radiative budget (EOS) (Wielicki et al., 1996, 1998) and aerosol abundance (Kahn et al., 2005; Levy et al., 2013b) to estimate the overall aerosol radiative effect (Christopher and Zhang, 2004; Patadia et al., 20~~ In particular, the sensitivitity of the aerosol direct radiative forcing to anthropogenic emissions remains uncertain. Previous work has shown that the aerosol forcing simulated by global climate models from 1850 to 2001 is well correlated with changes in $SO_2$ emissions (Stevens, 2015). However, ~~estimates of the aerosol forcing, the anthropogenic component of the aerosol effect, remain~~

primarily model based, as global observations cannot directly distinguish anthropogenic and natural aerosols (Su et al., 2013; Bellouin et al., 2005, 2008)this relationship may not be applicable in recent years and for future conditions, as the spatial distribution and speciation of anthropogenic emissions evolve (Stevens et al., 2017).

Here, we focus on the relationship between anthropogenic emissions and In this work, we aim to provide observational constraints on the sensitivity of the direct aerosol forcing (Stevens and Schwartz, 2012) and we examine whether significant changes in anthropogenic emissions over the key source regions of Europe, North America, China, and India over the 2001–2015 periods have affected the regional aerosol shortwave direct effect under clear-sky (SDRECS), where changes in SDRECS are to anthropogenic emissions. The paper is organized as follows First, we derive an estimate of changes in the clear-sky shortwave aerosol direct radiative effect from 2001 to 2015 constrained by the observed variability in outgoing shortwave radiation , surface albedo, ozone, and water vapor. A further motivation is from the Clouds and the Earth's Radiant Energy System (CERES). Second, we focus on large source regions of anthropogenic emissions (US, Europe, India, and Eastern China), where observed changes in the aerosol effect are expected to be dominated by anthropogenic aerosols. This allows us to assess whether a state-of-the-art chemistry climate chemistry-climate model (Geophysical Fluid Dynamic Dynamics Laboratory (GFDL) AM3) driven by the latest emission emissions from the Coupled Model Intercomparison Project (phase 6 ) can reproduce these observations. In particular, we show that the chemical speciation of SDRECS derived using AM3 can help understand differences in the regional response of SDRECS to emission changescan capture changes in the direct radiative forcing from aerosols over the 2001–2015 period. Finally we use AM3 to compare the sensitivity of the direct aerosol aerosol direct radiative forcing to emission changes from anthropogenic emissions from 1850 to 2001 and from 2001 to 2015 with the longer-term change between 1850 and 2001. 2015.

## 2 Methods

### 2.1 GFDL-AM3 model

We use the GFDL-AM3 model (Donner et al., 2011; Naik et al., 2013), the atmospheric chemistry climate component of the GFDL-CM3 model (Donner et al., 2011; Griffies et al., 2011; John et al., 2012). The model is run from 2000 to 2015, using the first year as spin-upto spin up the model. The model horizontal resolution is $\simeq$ 200 km with 48 vertical levels. To facilitate comparisons with synoptic observations, the model horizontal winds are nudged to 6-hourly horizontal winds from the National Centers for Environmental Predication reanalysis (Kalnay et al., 1996). Monthly sea surface temperature and sea ice concentration are prescribed following Taylor et al. (2000) and Rayner et al. (2003), respectively. The configuration of AM3 used in this study includes recent improvements to the representation of the wet scavenging of chemical tracers by snow and convective precipitation

(Liu et al., 2011; Paulot et al., 2016) and to the treatment of sulfate and nitrate chemistry (Paulot et al., 2016). We refer the reader to Paulot et al. (2016, 2017a) for detailed evaluation of this configuration of AM3.

The radiative transfer scheme takes into account the aerosol optical properties of sulfate, sea salt, dust, black carbon, organic carbon (Donner et al., 2011) and nitrate (Paulot et al., 2017b). Aerosols are assumed to be externally mixed, except for hydrophilic black carbon and sulfate (Donner et al., 2011). Hygroscopic growth is capped at 95% for all aerosols.

We use the anthropogenic emissions developed by the Community Emission Data System (CEDS v2017-05-18) for ~~the Coupled Model Intercomparison Project Phase 6 (CMIP 6 (Hoesly et al., 2018))~~CMIP6 (Hoesly et al., 2018). As anthropogenic emissions are available until 2014 from CEDS, we repeat CEDS 2014 anthropogenic emissions for 2015. Monthly biomass burning emissions are ~~based on the~~ from the historical global biomass burning emissions inventory for CMIP6 (BB4CMIP6, van Marle et al. (2017)). Emissions for the 1997 to 2015 period in this inventory have been derived from satellite-based emissions from the Global Fire Emissions Database ~~(van Marle et al., 2017) and distributed vertically following~~ (GFED, van der Werf et al. (2017)). The vertical distribution of biomass burning emissions is taken from Dentener et al. (2006). Natural emissions are based on Naik et al. (2013), except for isoprene emissions, which are calculated interactively using the Model of Emissions of Gases and Aerosols from Nature ~~(Guenther et al., 2006)~~(MEGAN, Guenther et al. (2006)).

Fig. 1 shows ~~regional and global trends~~ changes in the anthropogenic emissions of sulfur dioxide ($SO_2$~~,~~), ammonia ($NH_3$~~, BC, and NO~~ ), black carbon (BC), and nitrogen oxide (NO) from 2001 to 2015. Globally, anthropogenic emissions of $NH_3$, BC, and NO have increased by 18%, 36%, and 16% over the 2001-2015 period, respectively, while $SO_2$ emissions have remained nearly stable, peaking in 2006. In the US and Europe, there have been significant declines in $SO_2$ (-71% and -66%, respectively) and NO (-48% and -39%) emissions, while $NH_3$ and BC emissions have changed little (<15%). ~~In contrast, Chinese~~ Indian emissions of $SO_2$, NO, and BC have increased by ~~56%, 69~~89%, 39%, and ~~93%, respectively, while Indian~~ 89%. Similarly, Chinese emissions of $SO_2$, NO, and BC have increased by ~~89%, 39~~56%, 69%, and ~~89%. In India, ammonia emissions are larger relative to precursors of acidic aerosols (NO and $SO_2$)~~ 93%, respectively. Anthropogenic emissions in India and China are expected to be more uncertain than in the US and Europe ~~. Globally, emissions of $NH_3$, BC, and NO increase by 18%, 36~~(Saikawa et al., 2017a, b). For instance, Fig. 1 shows differences between emissions from CMIP6 and emissions from the regional Modular Emission Inventory for China (MEIC) (Zhang et al., 2009). Unlike in CMIP6, emissions of $SO_2$ decline starting in 2006, a decrease that accelerates in 2012, while NO emissions decrease after 2012 and BC emissions remain near-stable after 2007. In 2014, MEIC NO, $SO_2$, and BC emissions are 24%, 48%, and ~~16% over the 2001-2015 period~~32% lower than CMIP6 emissions, respectively. ~~$SO_2$ emissions are nearly stable, peaking in 2006.~~ $NH_3$ emissions are similar in magnitude but exhibit different seasonality: CMIP6 $NH_3$ emissions peak in spring, while MEIC exhibits a broad peak in summer,

consistent with top-down constraints (Paulot et al., 2014; Zhang et al., 2017). The impact of these emission uncertainties on the simulated change in the aerosol effect over India and China will be discussed in sections 3.2.2 and 3.2.3, respectively.

### 2.2 Aerosol optical depth

We use monthly aerosol optical depth (AOD) from the Multi-angle Imaging SpectroRadiometer (MISR) at 555nm (Kahn et al., 2005, 2010) and the Moderate Resolution Imaging Spectroradiometer (MODIS) instruments on board the AQUA and TERRA satellites at 550 nm (collection 6, level3, merged deep blue/dark target) (Levy et al., 2013a; Sayer et al., 2014). Because of our focus on interannual variability, we neglect diurnal variations in AOD ~~when comparing monthly model AOD with the different satellite products~~in the comparison with the simulated AOD.

### 2.3 Aerosol ~~shortwave~~ direct effect and forcing

The instantaneous aerosol direct radiative effect (DRE) is defined as the difference between the outgoing radiation ~~in the absence (Rutaf)~~ at the top of the atmosphere (TOA) in the absence and in the presence ~~(Rut) of aerosols at the top of~~ of aerosols (Heald et al., 2014). The direct radiative forcing (DRF) is defined as the anthropogenic component of the ~~atmosphere (TOA)~~direct radiative effect. In our notation we use the superscript $sw$ to denote the shortwave component of DRE or DRF. Likewise, the subscript $clr$ denotes the clear-sky component of DRE or DRF.

To better isolate the effect of aerosol variability on radiative fluxes, we will focus on the aerosol ~~direct shortwave~~ shortwave direct radiative effect under clear-sky conditions (~~SDRECS~~). DRE$^{sw}_{clr}$):

$$SDRECSDRE^{sw}_{clr} = Rsutcsaf - Rsutcsrsutcsaf - rsutcs \quad (1)$$

where ~~Rsutcs and Rsutcsaf~~ rsutcs and rsutcsaf are the outgoing clear-sky shortwave radiation with and without aerosols (http://clipc-services.ceda.ac.uk/dreq/index/CMORvar.html), respectively. For simplicity, we will refer to the aerosol shortwave direct radiative effect under clear-sky conditions (DRE$^{sw}_{clr}$) as the aerosol effect, hereafter. Note that an increase of ~~SDRECS~~ the aerosol direct effect indicates a decrease of the radiation scattered to space by aerosols.

#### 2.3.1 ~~Model-derived SDRECS~~Model

In AM3, ~~we estimate SDRECS~~ the aerosol effect is estimated by calling the radiative transfer scheme twice, with and without aerosols (Paulot et al., 2017b) in the absence of clouds. ~~Similarly, the instantaneous radiative effects~~ The effect of individual aerosol components ~~(SDRECS$_{\mathrm{AM3}}(x)$)~~ is estimated as the difference in ~~Rsut~~ outgoing shortwave radiation with and without aerosol $x$, where $x$ can be sulfate~~(SUL), nitrate(NIT)~~, nitrate, black carbon~~(BC)~~, organic carbon, dust, sea salt, and stratospheric volcanic aerosols. In the following, we will focus primarily on changes in sulfate and

nitrate, which dominate changes in aerosol scattering, and black carbon, which dominates changes in aerosol absorption ~~in AM3~~over the 2001–2015 period.

### 2.3.2 ~~Observation-based SDRECS~~Observations

~~In this section, we present three observation-based estimates of the variability in SDRECS from 2001 to 2015. All estimates described in this section are based upon the observed broadband radiance from the~~ The Clouds and the Earth's Radiant Energy System (CERES~~) (Wielicki et al., 1996, 1998).~~

~~A first estimate of SDRECS can be obtained using using equation (1) and the calculated Rsutcs and Rsutcsaf from the CERES Synoptic Radiative Fluxes product (SYN, edition 4a) . In CERES-SYN, both terms are calculated using a radiative transfer code constrained by the outgoing CERES TOA shortwave radiative flux (Rsut), and estimates for aerosol optical properties, precipitable water (WVP), and ozone (qo3). WVP and qo3 are from the Goddard Modeling and Assimilation Office (GMAO) GEOS5 reanalysis. Aerosol optical properties are from the Model for Atmospheric Transport and Chemistry (MATCH) model (Collins et al., 2001) constrained by MODIS AOD (collection 5). The CERES-SYN estimate of SDRECS will be referred to as $\mathrm{SDRECS_{CS}}$ hereafter.~~

~~A separate estimate of the variability in SDRECS can be derived using observations of Rsutcs from the CERES~~ , Wielicki et al. (1996, 1998)) provides constraints on the Earth's radiative budget since 2000. Here, we use the Energy Balanced and Filled product (EBAF, edition 4, ~~(Loeb et al., 2009))~~ Loeb et al. (2018)) to estimate the variability of the clear-sky shortwave outgoing radiation. This product achieves global coverage ~~for Rsutcs~~ by combining CERES broadband cloud-free fluxes with ~~estimates of Rsutcs from MODIS (at 1km resolution)~~ MODIS radiances for regions that are not completely cloud-free at the CERES footprint scale ~~(20 km) (CERES, 2017). We will use the subscript CE to refer to the CERES EBAF product hereafter.~~ (Loeb et al., 2018).

~~Rsutcsaf will contain changes dues to non-aerosol components (Stevens and Schwartz, 2012; Xing et al., 2015). Therefore, if we are to use equation (1) to estimate the variability in SDRECS, we need to estimate the variability in Rsutcsaf. Here we assume that that it is linearly related to the variability in surface albedo (salb), water vapor, and ozone column:~~

$$\Delta_{m,y}\left(Rsutcsaf\right) = \Delta_{m,y}((\alpha \cdot salb + \beta \cdot WVP + \gamma \cdot qo3) \cdot Rsdt)$$

~~where $\alpha = \frac{\partial palb}{\partial salb}$, $\beta = \frac{\partial palb}{\partial WVP}$ and $\gamma = \frac{\partial palb}{\partial qo3}$. Rsdt and palb are the incoming shortwave flux at the top of the atmosphere and the planetary albedo, respectively. $\Delta_{m,y}(x)$ is the anomaly in $x$ for month $m$ and year $y$ ($\Delta_{m,y}(x) = x_{m,y} - \frac{1}{15}\sum_{y=2001}^{2015} x_{m,y}$). Monthly gridded estimates of $\alpha$, $\beta$, and $\gamma$ are obtained from AM3.~~

~~We evaluate our methodology by showing that~~ The simplest way in which this data can be used to estimate changes in the aerosol effect is to assume that all variability in the shortwave clear-sky outgoing radiation is the result of changes in aerosols (Stevens and Schwartz, 2012; Xing et al., 2015; Alfaro-Contreras et al., 2017). We will refer to this estimate as $\mathrm{EBAF_R}$ hereafter (R: raw). However, other radiative components

may contribute to the variability in ~~Rsutcsaf calculated in SYN ($\mathrm{Rsutcsaf_{CS}}$) can be estimated using equation (??). Figure ?? shows the root mean square (RMS) of the annual anomaly in $\mathrm{Rsutcsaf_{CS}}$ (panel A) and how it is reduced by applying in succession the correction terms on the right hand side of equation ??. Correcting for~~ the outgoing radiation (Stevens and Schwartz, 2012). Therefore, a more accurate estimate of the aerosol effect requires removal of the impact of these components from the measured changes in the ~~salb reduces the RMS over most land regions (Figure ??B). However,~~ outgoing radiation. To achieve this, we estimate the variability of the outgoing clear-sky shortwave radiation associated with changes in surface albedo, ozone, and water vapor (see supporting materials and Fig. S1). For water vapor and ozone, we use the Goddard Modeling and Assimilation Office reanalysis (GEOS5). Since our estimate for the ~~RMS remains large over the Sahara, Australia, the Amazon, and North America. It is further reduced once changes in water vapor and to a lesser extend ozone are accounted for (Figure ??C and D). This gives us confidence in our ability to reproduce the variability in SDRECS calculated by the CERES SYN radiative transfer code when using the same albedo, water vapor , and ozoneas used in the CERES SYN calculations. However, CERES EBAF flux is measured and not calculated. Therefore the accuracy of our estimates for $\Delta_{\mathrm{m,y}}$Rstucsaf depends upon the accuracy of the estimates for surface albedo, water vapor, and ozone.~~

~~Figure ?? shows that $\Delta_{\mathrm{m,y}}$Rstucsaf~~ aerosol effect is most sensitive to ~~$\Delta_{\mathrm{m,y}}(\mathrm{salb})$, so we use two independent estimates of surface albedo derived from CERES EBAF ($\mathrm{salb_{CE}}$) and MODIS ($\mathrm{salb_{M}}$). The associated estimates of SDRECS will be denoted as $\mathrm{SDRECS_{CE}}$ and $\mathrm{SDRECS_{M}}$, respectively, hereafter. We use GEOS5 for WVP and qo3, similar to CERES SYN.~~ changes in the surface albedo, we will consider both the albedo from MODIS (Schaaf et al., 2002) and CERES-EBAF (Rutan et al., 2009, 2015; Loeb et al., 2018). Both albedo estimates have been validated extensively and generally show good agreement with observations (Cescatti et al., 2012; Wang et al., 2014b; Rutan et al., 2009, 2015). Estimates of the aerosol effect derived using the MODIS and CERES-EBAF albedo will be referred to as $\mathrm{EBAF_{M}}$ and $\mathrm{EBAF_{C}}$, respectively.

~~The MODIS albedo (MCD43C3) ($\mathrm{salb_{M}}$) (Schaaf et al., 2002) is derived using the estimated reflectivity of the surface in the absence of aerosols in 7 MODIS spectral bands (Vermote et al., 1997, 2002; Vermote and Saleous, 20 We use the estimates of the direct (black sky)and diffuse (white sky) albedo in both the near infrared and visible. Similar to Oleson et al. (2003), we consider the derived albedo regardless of the quality flag. The CERES surface broadband albedo ($salb_{CE}$) is estimated by finding the surface albedo that is most consistent with Rsutcs given constraints on aerosols from MATCH (Rutan et al., 2009, 2015), water vapor and ozone from GEOS5, and the spectral shape of the albedo. Both albedo estimates have been validated extensively and generally show good agreement with observations (Cescatti et al., 2012; Wang et al., 2014b; Rut~~ also use estimates of changes in the aerosol effect provided by the CERES Synoptic Radiative Fluxes product (SYN, edition 4a). The CERES SYN product calculates fluxes at the top of the atmosphere using a radiative transfer code constrained by observations. These calculations are performed with and without aerosols present, allowing for an estimate of the aerosol effect. The aerosol properties

used in the SYN calculations come from the Model for Atmospheric Transport and Chemistry (MATCH) that is constrained by observations from MODIS collection 5 (Collins et al., 2001). Therefore, the SYN calculated aerosol effect is very sensitive to MODIS collection 5 aerosol properties. This collection has now been superseeded by MODIS collection 6 (Levy et al., 2013b) and we will discuss some of the implications of differences between MODIS collections 5 and 6 for the derivation of the SYN aerosol effect in sections 3.2.1 and 3.2.2.

### 2.4 ~~Trend characterization~~

~~Trend significance is determined using~~

### 2.4 Trend identification

We use the non-parametric Mann-Kendall ~~$\tau$ at p=0.05 (Kendall, 1938)~~ test (Kendall, 1938) to identify significant changes in the aerosol effect. This test ~~is well-suited to the~~ quantifies monotonic correlations between two variables. It is based on a rank procedure that makes it less susceptible to outliers than the Pearson correlation and thus especially well-suited for the analysis of environmental ~~datasets as it does not require residuals to be normally distributed. When a significant trend is detected, we calculate~~ dataset. We estimate the linear trend using the Theil-Sen method (Theil, 1950; Sen, 1968). We use a critical $p$ value of 0.05 for trend significance.

## 3 Results

### 3.1 ~~Spatial distribution of changes in SDRECS~~

In this section, we will refer to the clear-sky shortwave outgoing radiation (rsutcs) and the aerosol shortwave direct radiative effect under clear-sky conditions ($\mathrm{DRE}^{\mathrm{sw}}_{\mathrm{clr}}$) as outgoing radiation and aerosol effect, respectively.

### 3.1 Global distribution of changes in aerosol effect

Fig. 2 shows the decadal rate of change in ~~outgoing shortwave radiation ($\mathrm{W\,m^{-2}\,dec^{-1}}$~~the aerosol effect, estimated solely from changes in the outgoing radiation ($\mathrm{EBAF_R}$) measured by CERES EBAF (top panel~~, plotted as -Rsutcs for consistency with the definition of SDRECS~~) over the 2001–2015 period. ~~Robust trends (dots) are detected~~ We find significant changes (highlighted with dots) in the outflow of the Eastern US~~(decrease in the shortwave radiation scattered to space)~~ , where the radiation scattered back to space by aerosols decreases, and in the outflow of India~~(increase in the shortwave radiation scattered to space), consistent with changes in aerosol precursors in these regions (~~, where it increases, consistent with the changes in anthropogenic emissions shown in Fig. 1~~)~~. However, ~~trends in Rsutcs are less robust and more heterogeneous~~ changes in the outgoing radiation are

less significant over the source regions themselves, which ~~suggests that other factors contribute to Rsutcs variability (Stevens and Schwartz, 2012; Xing et al., 2015)~~highlights the importance of other factors of variability in the outgoing radiation (Stevens and Schwartz, 2012).

Fig. 2 also shows the decadal rate of change in the ~~different observation-based estimates of SDRECS described in section 2.3.2 ($SDRECS_M$, $SDRECS_{CE}$, $SDRECS_{CS}$) . All~~ aerosol effect derived from the SYN calculation and from CERES-EBAF outgoing radiation after correction for water, ozone, and surface albedo from MODIS ($EBAF_M$) and CERES-EBAF ($EBAF_C$). All these estimates show better spatial consistency between land and ocean near large sources of anthropogenic pollution than ~~Rsutcs~~the outgoing radiation alone ($EBAF_R$). In particular, ~~they show a significant increase in SDRECS~~ we find that the aerosol effect increases over North America and Europe, and ~~a significant decrease~~ decreases over India. In contrast, ~~estimates of SDRECS show little variability~~ the variability is considerably reduced over Australia, ~~Kazakhstan~~Central Asia, and South America, which suggests that ~~the variability in Rsutcs~~ it is not primarily associated with aerosols~~in these regions.~~ . Consistent with observations, AM3 also shows ~~increases in SDRECS~~ that the aerosol effect increases over the US and Europe and decreases over India. However, it simulates a ~~large decrease in SDRECS~~ decrease in the aerosol effect over China and in the Western Pacific, which is inconsistent with observational ~~estimates~~constraints.

### 3.2 ~~Regional changes~~

~~Fig. 3 shows the annual anomalies in -Rsutcs (blue dashed line) and SDRECS (solid lines) over the Eastern US, Europe, India, and Eastern China. Rsutcs~~ To understand these changes further, we examine the timeseries of the different estimates of the aerosol effect over these regions. $EBAF_R$ exhibits considerable interannual variability over the Eastern US and Europe, with no significant trend (Table S1). In contrast, ~~all observational estimates of SDRECS~~ SYN, $EBAF_C$, and $EBAF_M$ estimates exhibit a significant increase ~~, i.e., a reduction of the radiation scattered to space by aerosols,~~ ranging from 0.9 to 1.8 $\mathrm{W\,m^{-2}\,dec^{-1}}$ in the Eastern US and from 0.7 to 1.4 $\mathrm{W\,m^{-2}\,dec^{-1}}$ in Western Europe. ~~The magnitude of the simulated trends in~~ AM3 also simulates an increase of the aerosol effect over these regions (0.8 and 0.6 $\mathrm{W\,m^{-2}\,dec^{-1}}$~~) are in good agreement with the estimates derived using MODIS surface albedo ($SDRECS_M$) but significantly lower than those derived from CERES-SYN ($SDRECS_{CS}$). This discrepancy will be discussed further in section 3.2.1~~ , respectively). The magnitude of these changes is in excellent agreement with $EBAF_M$ but lower than SYN. We refer the reader to section 3.2.1 for a detailed discussion of these regions.

Over India, ~~all observation-based estimates of SDRECS exhibit a significant decrease~~ most observational estimates (SYN, $EBAF_C$, $EBAF_M$) suggest a decrease of the aerosol effect ($-1.0$ – $-1.9\,\mathrm{W\,m^{-2}\,dec^{-1}}$), ~~i. e., an increase in the radiation scattered to space by aerosols. Unlike in the US and Europe, the simulated change in SDRECS (~~which is qualitatively captured by AM3 (-2.4 $\mathrm{W\,m^{-2}\,dec^{-1}}$). However, changes in the outgoing radiation alone ($EBAF_R$) would imply a small increase of the

aerosol effect from 2001 to 2015 (0.5 $\mathrm{W\,m^{-2}\,dec^{-1}}$)~~is in better agreement with $\mathrm{SDRECS_{CS}}$. Note that changes in -Rsutcs are opposite in sign to those of SDRECS. These contrasting trends~~ , which suggests that large changes in other radiative components may be masking the aerosol effect. Changes in the aerosol effect over India will be discussed ~~further~~ in section 3.2.2.

Over Eastern China, all observational estimates of ~~SDRECS all show~~ the aerosol effect exhibit a rapid decrease ~~of SDRECS~~ from 2001 to 2007, followed by an increase until 2015, with no significant trend overall in SYN, $\mathrm{EBAF_C}$, and $\mathrm{EBAF_M}$. The timing of the reversal is consistent with previous analysis of changes in AOD (Zhao et al., 2017) and ~~Rsutcs~~ outgoing radiation over the China sea (Alfaro-Contreras et al., 2017). AM3 fails to capture this reversal and simulates a significant decrease in ~~SDRECS~~ the aerosol effect from 2001 to 2015 (-1.3 $\mathrm{W\,m^{-2}\,dec^{-1}}$). Changes in ~~SDRECS~~ the aerosol effect over China will be discussed in section 3.2.3.

## 3.2 Regional changes

### 3.2.1 Western Europe and Eastern US

Fig. 4 ~~shows the observed and simulated seasonal changes in AOD and SDRECS over Western Europe. The first row shows the speciated AM3 AOD (bars) along with the~~ (top row) shows the seasonal change of the AOD and aerosol effect over Europe. Observations show that the AOD decreases most in spring and summer (-0.4 $\mathrm{dec^{-1}}$ for MODIS TERRA (solid black ~~), MODIS AQUA (cross), and MISR (diamond) AOD. For each season, AM3 is sampled where MODIS TERRA has valid observations for each month in the season. The second row shows the model-derived contribution of individual aerosol types to the overall SDRECS. The bottom row shows the annual anomaly in observation-based and model seasonal SDRECS.~~

~~Changes in AOD are dominated by spring and summer, with MODIS TERRA AOD decreasing -0.4 $\mathrm{dec^{-1}}$ in both seasons. Similarly, all estimates of SDRECS show increases of 1 to 1.8~~ line), Table 1). This decrease is accompanied by an increase of the aerosol effect of 1–1.8 $\mathrm{W\,m^{-2}\,dec^{-1}}$ in spring and 1.2~~to 2.5~~ –2.5 $\mathrm{W\,m^{-2}\,dec^{-1}}$ in summer (Fig. 4 (bottom row) and Table 1). ~~These changes are wellcaptured in AM3, where they~~ AM3 captures these changes well. In the model, both changes in AOD and aerosol effect are driven almost entirely by the decrease of sulfate aerosols associated with ~~declining~~ the decrease of $\mathrm{SO_2}$ emissions. The slower changes in winter and fall ~~can be attributed to~~ reflects the smaller contribution of sulfate to the aerosol burden and the ~~weaker response of sulfate to declining~~ less efficient oxidation of $\mathrm{SO_2}$ ~~emissions~~ in these seasons, which makes sulfate less sensitive to changes in $\mathrm{SO_2}$ emissions (Wang et al., 2011; Paulot et al., 2017a).

Fig. 5 shows the changes ~~in AOD and SDRECS~~ of the AOD and aerosol effect over the Eastern US. The overall pattern is ~~very~~ similar to Western Europe with large reductions in AOD (up to -0.11 $\mathrm{dec^{-1}}$) and increases in ~~SDRECS~~ the aerosol effect (up to 3.6 $\mathrm{W\,m^{-2}\,dec^{-1}}$) in spring and summer (Table 1). AM3 underestimates MODIS AOD as well as the rate of change of ~~SDRECS~~

~~and AOD (from all instruments)~~ the AOD and aerosol effect in summer (Table 1). This is consistent with the model low bias against ~~$SO_4^{2-}$~~ sulfate concentration in rain water in the US (Paulot et al., 2016). Similar to observations, AM3 also shows greater seasonal contrast between spring and summer in the US than in Europe. In the model, this is driven by more efficient springtime oxidation of $SO_2$ in Europe, where high emissions of ~~$NH_3$~~ ammonia facilitate its in-cloud oxidation by ozone (Paulot et al., 2017a).

~~Note that in~~ In both Europe and the US, ~~the magnitude and the trends of the MATCH AOD are greater than for MODIS (collection 6). These differences may be associated with~~ we find that the change in the aerosol effect inferred from the SYN calculation is larger than that estimated from CERES-EBAF outgoing radiation corrected for surface albedo changes ($EBAF_C$ and $EBAF_M$). The magnitude of the changes in the ~~MODIS AOD retrievals as MATCH uses the older~~ MATCH AOD, which is based on MODIS collection 5 ~~, and could explain the larger changes in $SDRECS_{CS}$ relative to $SDRECS_{CE}$~~ and ~~$SDRECS_M$~~ used to calculated the SYN aerosol effect, is also greater than that inferred from the improved MODIS collection 6 (Table 1). This suggests that the rate of change in SYN aerosol effect may be biased high in Europe and Western Europe.

### 3.2.2 India

Fig. 6 shows the changes in AOD and ~~SDRECS~~ aerosol effect over India. We will focus here on changes during the winter (DJF) and premonsoon seasons (MAM).

~~In winter, previous~~ Previous studies have shown that aerosols are primarily of anthropogenic origin in winter (Babu et al., 2013; Pan et al., 2015). During this season, all instruments show a significant increase in AOD (up to 0.13 $dec^{-1}$). ~~However, we find that the expected increase in Rsutcs is masked by a concomitant darkening of the surface~~ In spite of this increase, the outgoing radiation ($EBAF_R$) does not exhibit a significant trend. We attribute this apparent inconsistency to a concurrent decrease in surface albedo (Table S2), which may be associated with ~~increased~~ the increase in the regional greeness leaf area index ~~(LAI, Zhu et al. (2016)). We estimate that SDRECS decreased from 2001 to a 2015 at an average rate of~~ reported by Zhu et al. (2016). Accounting for changes in surface albedo, we diagnose a decrease in the aerosol effect ranging from -0.8 ~~–-2.8~~ $W\,m^{-2}\,dec^{-1}$ ~~. This large range reflects differences between the MODIS~~ (using MODIS albedo, $EBAF_M$) to -2.3 $W\,m^{-2}\,dec^{-1}$ (using CERES-EBAF albedo, $EBAF_C$). The large difference between $EBAF_C$ and ~~CERES salb products, with MODIS salb showing less rapid darkening~~$EBAF_M$ reflects the difference between MODIS and CERES-EBAF albedo in this region (Table S2).

~~Table 1~~ Fig. 6 shows that the simulated AOD agrees well for both magnitude and trend with MODIS AOD but overestimates the change in MISR ~~and MATCH AOD . The large difference between MODIS and MATCH AOD may also be associated with changes in LAI as the effect of vegetation on surface reflectivity was revised in collection 6 (Levy et al., 2013b). AM3 falls at the upper end of observational estimates for SDRECS~~ AOD (see also Table 1). The simulated change

in the aerosol effect (-2.7 $\mathrm{W\,m^{-2}\,dec^{-1}}$) ~~, in good agreement with $\mathrm{SDRECS_{CS}}$ (~~agrees well with the $\mathrm{EBAF_C}$ and SYN estimates (-2.3 and -2.6 $\mathrm{W\,m^{-2}\,dec^{-1}}$, respectively). However, ~~the agreement with $\mathrm{SDRECS_{CS}}$ is fortuitous~~this good agreement is fortuitous, as the higher surface albedo in AM3 (0.166) relative to ~~CERES-SYN~~ SYN (0.129) or CERES-EBAF (0.135) tends to dampen changes in the simulated aerosol scattering. ~~We calculate that the lower albedo in CERES-SYN would amplify the simulated trend by -0.8~~ Specifically, we estimate that the simulated trend in the aerosol effect would be -3.5 $\mathrm{W\,m^{-2}\,dec^{-1}}$ if AM3 was forced with the SYN albedo. This suggests that AM3 overestimates the decrease in ~~SDRECS~~ the aerosol effect by 1 to 2 $\mathrm{W\,m^{-2}\,dec^{-1}}$.

~~The model high biasfor the rate of change in SDRECS may reflect insufficient aerosol absorption or excessive aerosol scattering. Table 1 shows that black carbon~~ Many factors could contribute to this bias. Here we focus on the seasonality of the emissions of black carbon and ammonium nitrate precursors. Black carbon is the largest contributor to aerosol absorption over India (+3.2 $\mathrm{W\,m^{-2}}$ on average in winter). Its increase cancels out one third (0.9 $\mathrm{W\,m^{-2}\,dec^{-1}}$) of the decrease in ~~SDRECS~~the aerosol effect, much more than in the US and Europe. This is likely to be an underestimate as the prevalent use of biofuel in winter for heating, a large source of ~~BC (Pan et al., 2015)~~black carbon (Yevich and Logan, 2003; Pan et al., 2015), is not represented in the CMIP6 emission inventory. ~~Table 1 also shows that the increase of nitrate aerosols is the dominant driver for SDRECS change~~ Nitrate dominates changes in the aerosol scattering in winter (-2.4 $\mathrm{W\,m^{-2}\,dec^{-1}}$). This is consistent with previous multi-model assessments, which showed that models that did not include nitrate severely underestimated the AOD over India (Pan et al., 2015). Nitrate is formed via the reaction of ammonia (primarily from agriculture) and nitric acid (from the oxidation of NO, whose emissions are dominated by fossil fuel combustion). ~~In the CMIP6 emission inventory~~Nitrate remains challenging to represent in models because of uncertainties in both ammonia emissions and its chemistry and removal (Heald et al., 2012; Paulot et al., 2016). In particular, the seasonality of Indian ammonia emissions in ~~India follows that of Europe, with a~~ CMIP6 is based on European emissions and peak in spring. ~~We conducted a sensitivity simulation using the seasonality of $\mathrm{NH_3}$ column from AIRS (Warner et al., 2017) to modulate $\mathrm{NH_3}$ emissions. We find that this revised seasonality significantly reduces the simulated winter trend in SDRECS (0.08~~ In contrast, Warner et al. (2017) recently showed that the ammonia column peaks in summer over India (Fig. S2). Using AM3, we estimate that modulating ammonia emissions with the seasonality derived from satellite would reduce the simulated trend in the aerosol effect in winter from -2.7 to -1.9 $\mathrm{W\,m^{-2}\,dec^{-1}}$~~), improving the agreement with observations~~. These suggest that uncertainties in the seasonalities of black-carbon and ammonia emissions alone could explain most of the discrepancy between observed and simulated changes in the wintertime aerosol effect.

In the premonsoon season, ~~Fig. 6 shows that~~ the AOD changes much less rapidly than in winter (Fig. 6, Table 1). For instance, MODIS (TERRA) AOD increases by 0.04 $\mathrm{dec^{-1}}$~~in MAM~~, less than a third of the rate in winter. ~~In contrast ,~~ This seasonal contrast is not captured by AM3~~simulates an~~

increase in AOD of , which simulates a similar change (0.15 $dec^{-1}$, similar to the rate of change in winter $dec^{-1}$) in both seasons (Table 1). We also find a significant decrease (This discrepancy can be partly explained by the decrease of dust optical depth (dash black line, -0.07 $dec^{-1}$) in the MODIS-derived dust optical depth (Ginoux et al., 2012), consistent with the decline in diagnosed from MODIS folowing Ginoux et al. (2012). This decline, which is not captured by AM3, is supported by the decline of coarse-mode aerosols in the Indo-Gangetic Plain (IGP, Babu et al. (2013)). This (Babu et al., 2013). Using the simulated relationship between dust optical depth and dust aerosol effect, we estimate that the reduction in dust optical depth has caused an increase in the aerosol effect of 1.4 $W m^{-2} dec^{-1}$. This suggests that the decline of dust is not captured by AM3 and could account accounts for most of the discrepancy between model and simulated AOD trends. Such decrease in dust would also reduce the magnitude of the change in SDRECS from the model (-3.1 to -1.7 $W m^{-2} dec^{-1}$, in better agreement with the observation-based range of ) and the observational estimates of changes in the aerosol effect (-0.9 – -1.4 $W m^{-2} dec^{-1}$. To our knowledge, the mechanism for this decrease of dust over India in spring has not been identified. Babu et al. (2013) reported that the GOCART model, which uses the same dust emission parameterization as AM3 (Ginoux et al., 2001), but includes modulation ).

Jin and Wang (2018) recently suggested that higher precipitation in Northwestern India has caused a regional greening, which has been accompanied by a reduction of dust emissions. This mechanism may explain why the Goddard Chemistry Aerosol Radiation and Transport (GOCART), which includes the modulation of dust emissions by LAI (Kim et al., 2013), captures the decrease of dust in this region (Babu et al., 2013). This suggests that the impact of soil bareness by vegetation (Kim et al., 2013), does exhibit a decrease in the dust burden in the IGP. More studies are clearly needed to better understand the cause of the LAI increase in India and its connection with surface darkening and the decrease of spring dust, as both these processes have masked the impact of increasing anthropogenic aerosols on the outgoing shortwave radiation radiation may have been masked by regional greening both directly (via the decrease of the surface albedo) and indirectly (via lower dust emissions).

### 3.2.3 Eastern China

Fig. 7 shows the change in AOD and SDRECS aerosol effect over Eastern China. AM3 captures the average magnitude of AOD well in winter and spring but underestimates AOD (MODIS) during the monsoon and post monsoon seasons (Table 1). Although there are significant differences between the different AOD retrievals (Zhao et al., 2017), no homogeneous significant trend is detected in either AOD or SDRECS over the aerosol effect over the entire 2001-2015 period in any season. Note that recent studies show that MODIS AOD is biased high against ground-based observations in China (Tao et al., 2015; Xiao et al., 2016), which may be associated with the representation of surface properties in the retrieval algorithm (Wu et al., 2016).

In contrast to observations, ~~AM3 exhibits a large positive trend in AOD and negative trend in SDRECS in~~ simulated AOD and aerosol effect exhibit significant changes in both spring (0.15 $\mathrm{dec}^{-1}$ and -2.1 $\mathrm{W\,m^{-2}\,dec^{-1}}$, respectively) and summer (0.11 $\mathrm{dec}^{-1}$ and -1 $\mathrm{W\,m^{-2}\,dec^{-1}}$, respectively). ~~Changes are greatest in spring, when large emissions of $NH_3$ favor both the production of nitrate and sulfate (via in-cloud oxidation by ozone) aerosols. Sulfate~~ In spring, sulfate is the largest contributor to the AOD and ~~SDRECS in spring,~~ aerosol effect but changes are dominated by ~~the increase of~~ nitrate aerosols (0.08 $\mathrm{dec}^{-1}$ and -2.2 $\mathrm{W\,m^{-2}\,dec^{-1}}$, respectively (Table 1). This large springtime change in nitrate is associated with the May maximum of ammonia emissions in the CMIP6 emission inventory.

Similar to India, ~~this~~ the model bias may be associated with uncertainties in anthropogenic emissions. ~~Fig. 1 shows that Chinese $SO_2$ emissions in~~ As noted in section 2.1, there are significant differences between the CMIP6 ~~emission inventory are nearly stable~~ and MEIC emission inventories for $SO_2$ after 2007 ~~, while NO and BC emissions increase until~~ and NO after 2013 ~~before stabilizing. In contrast, the Modular Emission Inventory for China (MEIC), a regional inventory, designed to take into account the impact of rapid technological and regulatory changes on emissions (Zhang et al., 2009), shows a decline of $SO_2$ emissions starting in 2006 and accelerating in 2012, a decrease of NO after 2012, and near-stable BC emissions after 2007. In 2014, MEIC NO, $SO_2$, and BC emissions are 24%, 48%, and 32% lower than CMIP6 emissions, respectively. $NH_3$ emissions are similar in magnitude but exhibit different seasonality. CMIP6 $NH_3$ emissions peak in spring, while MEIC exhibits a broad peak in summer, which is supported by top-down constraints (Paulot et al., 2014; Zhang et al., 2017).~~ (Fig. 1). A detailed evaluation of these two emission inventories is beyond the scope of this study. However, observations show significant declines in $SO_2$ columns starting in 2008 (Li et al., 2010; Irie et al., 2016; de Foy et al., 2016; Liu et al., 2016; Ding et al., 2017; van der A et al., 2017; Krotkov et al., 2016) and $NO_2$ starting in 2012 (Liu et al., 2016; van der A et al., 2017), ~~which is~~ consistent with MEIC ~~trends~~emissions. We refer the reader to the ~~recent~~ study of van der A et al. (2017) for a detailed discussion of the technological and regulatory changes that have contributed to the changes in Chinese emissions over the 2001-2015 period.

~~In order to assess the impact of these revised emissions on the simulated AOD and SDRECS~~To quantify the sensitivity of our results to these uncertainties, we perform ~~a sensitivity simulations using MEIC~~ another simulation replacing the CMIP6 emission by the MEIC emissions for NO, BC, $SO_2$, ~~$NH_3$ and NO emissions for China(Fig. S1).~~ and $NH_3$ over China. We find that ~~MEIC emissions reduce the simulated AOD trend~~ the reduction of $SO_2$ emissions after 2007 reduces the the simulated trend in springtime AOD by 40% ~~in spring primarily through reduction in sulfate aerosols. The change in the SDRECS trend is smaller (-15%)as opposite changes in SDRECS(BC) and SDRECS(SUL) offset each other. This small reduction does not improve the simulated annual trend (-1.8 $\mathrm{W\,m^{-2}\,dec^{-1}}$), as higher emissionsof ammonia in winter and fall result in higher sulfate and nitrate in these seasons, in spite of lower NO and~~ from 0.15 $\mathrm{dec}^{-1}$ to 0.09 $\mathrm{dec}^{-1}$ in better

agreement with observations (Fig. S3). In contrast, the simulated trend of the springtime aerosol effect changes by less than 15% relative to the simulation driven by CMIP6 emissions. This primarily reflects the decrease of both black carbon and $SO_2$ ~~emissions~~emissions starting in 2007 (Fig. 1), which results in opposite changes in the aerosol effect.

~~The lack of sensitivity of sulfate to $SO_2$ emissions reflects strong oxidant limitations in AM3 (Paulot et al., 2017a). However, recent~~ Errors in the representation of the photochemical production of aerosols may also contribute to the model bias. Recent studies have shown that the ~~oxidation pathways of $SO_2$ represented in AM3, e.g., homogeneous oxidation by OH and aqueous oxidation by $O_3$ and $H_2O_2$, can not sustain the observed concentrations of sulfate in the North China Plains (Wang et al., 2014a; Zheng et al., 2015). Under hazy conditions,~~ heterogeneous oxidation of $SO_2$ by $NO_2$ (Cheng et al., 2016) ~~or~~ and $O_2$ (Hung and Hoffmann, 2015) at the surface of or in aerosols may be ~~the dominant sources of $SO_4^{2-}$, although the relative importance of these pathways remains uncertain (Guo et al., 2017; He et al., 2017). In order to quantify~~ an important source of sulfate in the North China Plains (Wang et al., 2014a; Zheng et al., 2015; Guo et al., 2017; He et al., 2017). To examine the sensitivity of our ~~results to these reactions~~simulation to this chemistry, we perform an additional simulation using MEIC emissions and the parameterization of the ~~uptake coefficient of $SO_2$ on aerosols derived by Zheng et al. (2015) :~~

~~Fig. **??** shows~~ heterogeneous production of sulfate on aerosols from Zheng et al. (2015) (Fig. S4). We find that the heterogeneous oxidation of ~~$SO_2$~~ sulfate increases the simulated sulfate optical depth by 100% in winter and 62% in fall~~. Changes~~ , relative to the simulation driven by MEIC emissions. In contrast, changes are much smaller ($< 25\%$) in spring and summer, ~~because of greater oxidant availability~~ which reflects the greater availability of oxidants. The increased production of sulfate in winter and fall results in a stronger link between $SO_2$ emissions and the simulated AOD and ~~SDRCES. This~~ aerosol effect (Fig. S4). This stronger link allows the model to better capture some prominent features in the observational record, such as the ~~SDRECS dip and AOD peak in~~ dip in the aerosol effect in fall 2006 ~~, as well as the decrease in AODand increase in SDRECS~~ (peak in AOD) or the AOD decrease after 2013. ~~However, on an annual basis, the simulated decrease in SDRECS remains biased high relative to observations, as~~ This suggests that both changes to the CMIP6 emissions and to the representation of $SO_2$ photochemistry are needed for AM3 ~~does not capture the increase in SDRECS from 2007 to 2015 (not shown).~~ to capture observed changes in the aerosol effect over China from 2001 to 2015.

## 4 Implication for the aerosol direct forcing

~~The aerosol direct forcing (DRF, Heald et al. (2014)) is a measure of the change in DRE associated with anthropogenic emissions since preindustrial time (taken here as 1850).~~ In section 3.2, we have shown that regional differences in the speciation of anthropogenic emissions ~~and~~ (e.g., the ratio of

ammonia and BC to $SO_2$) and the oxidative environment are important to understand changes in ~~SDRECS~~ the direct shortwave aerosol radiative effect under clear-sky over the largest sources of anthropogenic pollution. ~~Here, we examine whether these changes have changed the sensitivity of DRF to anthropogenic emissions .~~

~~To examine this issue, we compare changes in simulated all-sky~~ Fig. 8 shows that the changes in the meridional distribution of BC, NO, $NH_3$ and ~~clear-sky direct radiative forcing (DRF and DRFCS, respectively)for two time periods,~~ $SO_2$ anthropogenic emissions between 1850 ~~to 2001~~ and 2001 ~~to 2015. We estimate the DRF for~~ (panel a) and between 2001 and ~~2015 as~~2015 (panel b). In particular, the 2001–2015 period is characterized by higher emissions of BC (25%), NO (15%), and $NH_3$ (19%) and lower $SO_2$ emissions (-12.5%), relative to the 1850–2001 period. While BC and $NH_3$ emissions have increased in most regions, the change in $SO_2$ and NO emissions is associated with a decline in the northern midlatitudes and an increase in the tropics. Here, we quantify the associated changes in the meridional distribution of the aerosol direct radiative forcing (DRF), the anthropogenic component of the aerosol direct radiative effect.

The aerosol direct radiative forcing for year $y$ is calculated as:

$$DRF(y) = DRE(anthro = y, met = y) - DRE(anthro = 1850, met = y) \quad (2)$$

where $anthro$ and $met$ denote the year used for anthropogenic emissions and to nudge the horizontal wind, respectively. Note that we use the same meteorology for both simulations, in order to minimize differences in natural sources (e.g., dust, seasalt, dimethylsulfide). ~~Following the AEROCOM practice (Myhre et al., 2013), we do not consider biomass burning as part of the anthropogenic emissions.~~ On the basis of our evaluation of AM3, we include MEIC emissions for China, ~~revised~~ the seaonality of $NH_3$ ~~seasonality~~ from AIRS in India, and the heterogeneous oxidation of $SO_2$ on aerosol surfaces.

~~Fig. 8 (panels a and b) shows the meridional changes in anthropogenic emissions of BC, NO, $NH_3$ and $SO_2$ between~~ We estimate the forcing from biomass burning and non-biomass burning sources separately, as the contribution of anthropogenic activities to changes in biomass burning emissions remains uncertain (Heald et al., 2014). The average 2001–2015 simulated direct radiative forcing from fires is -0.011 $\mathrm{W\,m^{-2}}$, which falls within the range of previous model assessments ($0.0 \pm 0.05 \mathrm{W\,m^{-2}}$, (Myhre et al., 2013)) . In the following we focus on the radiative forcing from non-biomass burning sources from 1850 ~~and~~ to 2001 ~~(a) and 2001~~ and ~~2015 (b). The overall change in BC, NO, and $NH_3$~~ from 2001 to ~~2015 are 25%, 15%, and 19% of their change from 1850 to 2001. In contrast, $SO_2$ emissions have been reduced by 12.5%. From 2001 to 2015, BC and $NH_3$ have increased in most regions, while both $SO_2$ and NO emissions have declined in the northern midlatitudes but increased in the tropics.~~ 2015.

~~Changes in the DRFCS (~~

### 4.1 Clear-sky aerosol direct radiative forcing

The aerosol clear-sky direct radiative forcing in 2001 relative to 1850 is -0.64 $\mathrm{W\,m^{-2}}$, which agrees well with previous assessments (Table S3). This forcing is dominated by changes in sulfate (-0.73 $\mathrm{W\,m^{-2}}$), which are partly offset by changes in BC (+0.36 $\mathrm{W\,m^{-2}}$). Fig. 8c ~~) of individual aerosols from 1850 to~~ shows that the meridional distribution of the clear-sky radiative forcings of individual aerosols in 2001 ~~largely mirror the emissions~~ relative to 1850 largely mirror that of their precursors' emissions. Some deviations can be noted however. For instance, ~~DRFCS(BC)~~ the forcing from black carbon is enhanced at high latitudes because of ~~high~~ the higher surface albedo (Myhre et al., 2013)~~), while the broader latitudinal extend of DRFCS(SUL) relative to $SO_2$ emissions is partly associated with the less efficient oxidation of $SO_2$ over large source regions (Fig. S2).~~ .

~~The overall DRFCS decreases by -0.64 $\mathrm{W\,m^{-2}}$ from 1850 to 2001, which agrees well with previous assessments (Table S3). Changes in DRFCS reflect the competing effects of changes in $SO_4^{2-}$ (DRFCS(SUL) = -0.73 $\mathrm{W\,m^{-2}}$) and BC (DRFCS(BC)=0.36 $\mathrm{W\,m^{-2}}$). DRFCS changes little between 2001 and~~ We find little change in the aerosol clear-sky direct radiative forcing in 2015 relative to 2001 (-0.04 $\mathrm{W\,m^{-2}}$) consistent with previous studies (Murphy, 2013; Kühn et al., 2014). In AM3, this reflects the ~~near~~ cancellation between the ~~increase in DRFCS in~~ positive clear-sky aerosol direct radiative forcing in the northern midlatitudes (associated with the decrease of sulfate and the increase of BC) and the ~~decrease of DRFCS~~ negative clear-sky aerosol direct radiative forcing in the northern tropics (associated with the increase of nitrate and sulfate aerosols).

~~The change of DRFCS(BC) from 2001 to~~ Next we examine the sensivitiy of indivual forcings to anthropogenic emissions in both periods. The clear-sky direct radiative forcing of black carbon in 2015 relative to 2001 is 25% of the ~~change from 1850 an~~ forcing in 2001 relative to 1850, in good agreement with the change in BC emissions. In contrast, the ~~relationship between DRFCS(SUL) (~~clear-sky direct radiative forcing of sulfate changes little between 2001 and 2015 (+3%)~~and changes in ~~, while $SO_2$ emissions ~~(~~decline by -12.5% ~~) is different from the 1850–2001~~ over the same time period. This ~~primarily reflects~~ small change in the sulfate forcing reflects the cancellation between opposite changes in the tropics, where the forcing from sulfate aerosols is negative, and the midlatitudes, where it is positive. AM3 shows a stronger sensitivity of the sulfate forcing to changes in $SO_2$ emissions in the tropics than in the midlatitudes. This difference can be attributed to regional differences in the oxidative environment~~(Fig. S2), with greater conversion efficiency ~~, as a) greater actinic flux allows for more efficient oxidation of $SO_2$ ~~to $SO_4^{2-}$~~ in the tropics ~~, where $SO_2$ emissions increase,~~ than in the midlatitudes ~~, where they decrease. Furthermore, the fraction of~~ (Fig. S4), and b) the efficiency of the oxidation of $SO_2$ ~~molecules oxidized to $SO_4^{2-}$~~ to sulfate tends to increase with decreasing $SO_2$ emissions, as oxidant limitations become less important~~. This tends to dampen the response of DRFCS(SUL) to the decrease of~~ , which diminishes the sensitivity of sulfate to changes in $SO_2$ emissions in the midlatitudes ~~(Paulot et al., 2017a). Similar~~ (Fig. S4).

In contrast to sulfate, the change in ~~DRFCS(NIT) (~~the clear-sky direct radiative forcing from nitrate from 2001 to 2015 (+75%) is ~~different from the changes~~ greater than the change in the emissions of ~~nitrate precursors ($NH_3$~~ its precursors (ammonia and NO emissions increase by less than 20%). ~~This higher sensitivity reflects in part the~~ The higher sensitivity of nitrate to emission changes in the 2001-2015 period is consistent with the decrease of sulfate in the northern midlatitudes, which enables more ammonia to react with nitric acid to produce ammonium nitrate (Ansari and Pandis, 1998). In ~~addition, the magnitudes of both DRFCS(NIT) and DRFCS(SUL) increase in the tropics, which reflects the higher ratio of $NH_3$~~ the tropics, ammonia is less limiting (the ratio of ammonia to $SO_2$ emissions ~~in this region.~~ is higher) and the magnitude of both nitrate and sulfate forcings are simulated to increase from 2001 to 2015.

### 4.2 All-sky aerosol direct radiative forcing

Clouds can enhance the reflectivity of the surface beneath aerosols as well as mask the effect of aerosols underneath (Heald et al., 2014). Overall, clouds tend to amplify the forcing of absorbing aerosols and diminish that of scattering aerosols. The simulated ~~DRF(~~aerosol forcing in 2001 ~~)~~ is -0.09 $\mathrm{W\,m^{-2}}$, at the low end of previous multi-model assessments (-0.27 $\pm$0.15$\mathrm{W\,m^{-2}}$ (Myhre et al., 2013) and Table S2) switching sign from negative to positive North of 45°. For comparison, the instantaneous radiative forcing from well-mixed greenhouse gases at TOA, as calculated from the GFDL Standalone radiation code (Schwarzkopf and Ramaswamy, 1999; Freidenreich and Ramaswamy, 1999), is +1.84 $\mathrm{W\,m^{-2}}$ in 2001.

From 2001 to 2015, ~~DRF~~ the direct aerosol forcing is simulated to ~~increase by~~ be +0.03 $\mathrm{W\,m^{-2}}$ ~~and 0.27~~, including +0.12, -0.03, and -0.03 $\mathrm{W\,m^{-2}}$ from ~~aerosols and well-mixed greenhouse gases~~black carbon, sulfate, and nitrate, respectively. ~~In the northern midlatitudes, the decrease of sulfate and the increase in black carbon are simulated to increase the regional direct radiative forcing by up to 0.25 $\mathrm{W\,m^{-2}}$ , which is comparable to the forcing~~ Myhre et al. (2017) recently reported a similar change in the overall direct radiative forcing (+0.01 $\mathrm{W\,m^{-2}}$) but different contributions from sulfate (+0.03 $\mathrm{W\,m^{-2}}$) and black carbon (+0.03 $\mathrm{W\,m^{-2}}$). Many factors could contribute to these differences including the radiative properties of aerosols (e.g., the mixing of sulfate with black carbon (Bond et al., 2013)) and the emission inventories. Further studies are needed to examine whether changes in the sensitivity of radiative forcing to anthropogenic emissions are robust across models. Such assessment would be especially important in the northern midlatitudes, where the direct radiative forcing from aerosols and greenhouse gases from ~~greenhouse gases. This highlights the need to account for aerosols to characterize recent regional changes in radiative forcing.~~ 2001 to 2015 are simulated to be of similar magnitude (+0.25 $\mathrm{W\,m^{-2}}$).

## 5 Conclusions

We have ~~used observations of the outgoing shortwave radiation and the variability~~ derived estimates of the changes in the aerosol direct clear-sky shortwave radiative effect from 2001 to 2015 using variations in the outgoing shortwave clear-sky radiation from CERES-EBAF. Even over polluted regions, such changes can not be solely ascribed to aerosols and the impact of changes in surface albedo, ~~ozone, and water vapor to estimate changes in the aerosol shortwave direct effect under clear sky (SDRECS) from 2001 to 2015.~~ water vapor and ozone on outgoing radiation need to be accounted for. In particular, we have shown that the effect of increasing anthropogenic aerosols on the outgoing radiation has been largely masked by a decrease in surface albedo over India.

We ~~use these observational constraints~~ have used observed seasonal changes in AOD and aerosol effect over large source regions of ~~pollution to evaluate~~ anthropogenic emissions to assess the representation of anthropogenic emissions and their impact on atmospheric chemistry and ~~radiative forcing~~ the aerosol direct radiative effect in the GFDL-AM3 ~~chemistry climate model.~~ global chemistry-climate model. Such observational constraints may be especially valuable for future multi-model assessments.

Our work suggests a mature understanding of changes in the aerosol effect over the US and Europe, ~~which are dominated by the ongoing decrease of $SO_2$ sources.~~where the decrease of sulfate aerosols accounts for most of the increase (i.e., the weakening) in the aerosol direct clear-sky shortwave radiative effect. In contrast, the different mix of anthropogenic emissions in India and China results in a more complex speciation of ~~SDRECS~~aerosols responsible for changes in the aerosol direct effect, with large contributions from sulfate, nitrate, and black carbon. ~~These~~ Trends in these regions remain challenging to capture in the GFDL AM3 ~~. First, we find significant uncertainties in the CMIP6 emissions, including in the seasonality of $NH_3$, which is based on agricultural practices in Europe, and in the seasonality of black carbon , which is neglected in India. The reduction of Chinese anthropogenic emissions of $SO_2$ and NO after 2007 is also underestimated and results in an excessive decrease in SDRECS over China and the Western Pacific. Second, differences in regional photochemistry result in different sensitivity of SDRECS to anthropogenic emissions in China and India compared to the Eastern US and Europe. In particular, the competition for ammonia between~~ model. Some of these biases may be model-specific, including the treatment of the mixing between sulfate and black carbon or the representation of the photochemistry of sulfate and nitrate~~tends to limit the formation of nitrate in the US and Europe. In contrast, in India, larger emissions of both ammonia and nitrogen oxide enables both sulfate and nitrate to increase from 2001 to 2015. In addition,~~ . Others are attributed to the CMIP6 emissions and will likely affect other models. In particular, we find that the model ~~better captures the variability in SDRECS over China, when accounting for the heterogeneous oxidation of~~ bias in winter over India can be largely accounted for by uncertainties in the seasonality of ammonia and black carbon emissions. Similarly, comparisons between the CMIP6 and MEIC emission inventories over China suggest that the model bias in this

region can be largely attributed to an underestimate in CMIP6 of the reduction of $SO_2$ ~~on aerosols, a reaction that has little impact on the sulfate budget in Europe and the US.~~ emissions after 2007.

~~We find that even over regions of high anthropogenic emissions, changes in Rsutcs are not necessarily associated with changes in anthropogenic aerosols. In particular, in India, a darkening of the surface, possibly associated with an increase in LAI, and a decline in dust sources may have masked much the anthropogenic signal in Rsutcs over the 2001-2015 period.~~

~~Clearly more work is needed to further characterize the regional speciation of SDRECS and its sensitivity to changes in anthropogenic emissions . In particular~~Our study shows that regional differences in the emission mix and oxidative conditions have a large impact on the relationship between anthropogenic emissions and direct aerosol forcing. Specifically, we have shown that ~~it is important to account for~~ changes in the ~~ratio of~~ magnitude, speciation, and spatial distribution of anthropogenic emissions have dampened the sensitivity of the aerosol forcing to $SO_2$ ~~to BC emissions and for non-linearities in nitrate and sulfate chemistry to understand recent changes in DRF. Therefore, attempts to describe DRF, simply as a function~~ emissions, but amplified that to emissions of NO and ammonia, the precursors of nitrate aerosols. This suggests that relationships between anthropogenic emissions and aerosol forcing derived over the 1850–2001 period and thus largely controlled by changes of $SO_2$ in Europe and North America (Stevens and Schwartz, 2012) need to be revisited ~~(Stevens et al., 2017)~~with an emphasis on black carbon and ammonia in Asia.

*Acknowledgements.* We thank the many researchers, who have contributed to the CERES, MODIS, and MISR products used in this study. CERES data were obtained from the NASA Langley Research Center CERES ordering tool at http://ceres.larc.nasa.gov/. MODIS albedo (MD43C3 MODIS/Terra+Aqua BRDF/Albedo Albedo Daily L3 Global 0.05 Deg CMG V006) was obtained in netCDF file format from the Integrated Climate Data Center (ICDC, http://icdc.cen.uni-hamburg.de, University of Hamburg, Hamburg, Germany). MISR and MODIS AOD products can be obtained from the NASA Earthdata portal. Model outputs are available upon request to Fabien.Paulot@noaa.gov. We thank Drs ~~Bo Zheng and Qiang~~ B. Zheng and Q. Zhang for providing MEIC gridded emissions. This work was supported by NOAA Climate Program Office. P. G. acknowledges partial funding by NASA through NNH14ZDA001N-ACMAP grant. We thanks Dr A. Jones~~and~~ , Dr. L.J. Donner, and two anonymous reviewers for helpful comments. All figures were generated using the NCAR Command Language (Version 6.4.0, http://dx.doi.org/10.5065/D6WD3XH5).

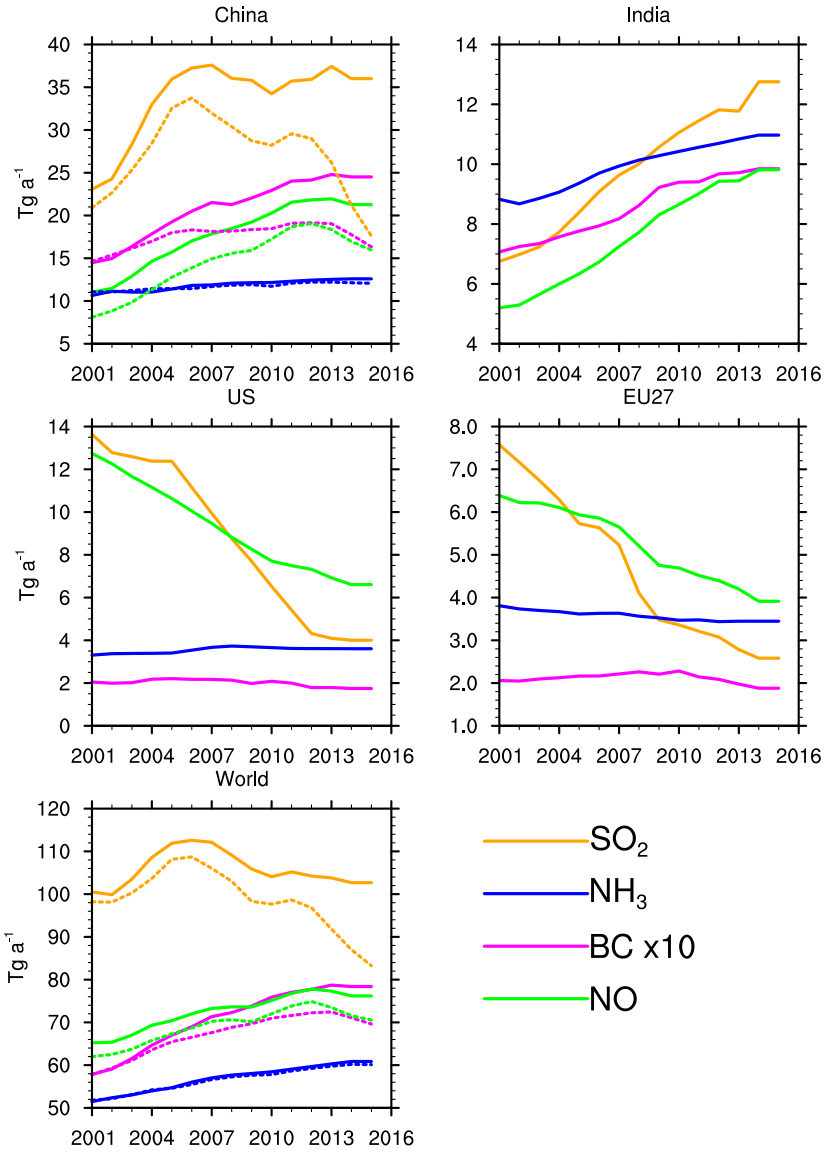


**Figure 1.** Annual anthropogenic emissions of $SO_2$, BC, $NH_3$, and NO from ~~CEDS~~ CMIP6 (solid lines) in selected regions. Emissions of $SO_2$, and NO with anthropogenic emissions from MEIC (for agriculture, energy, transportation, industry, and residential sectors) are also shown (dash lines).

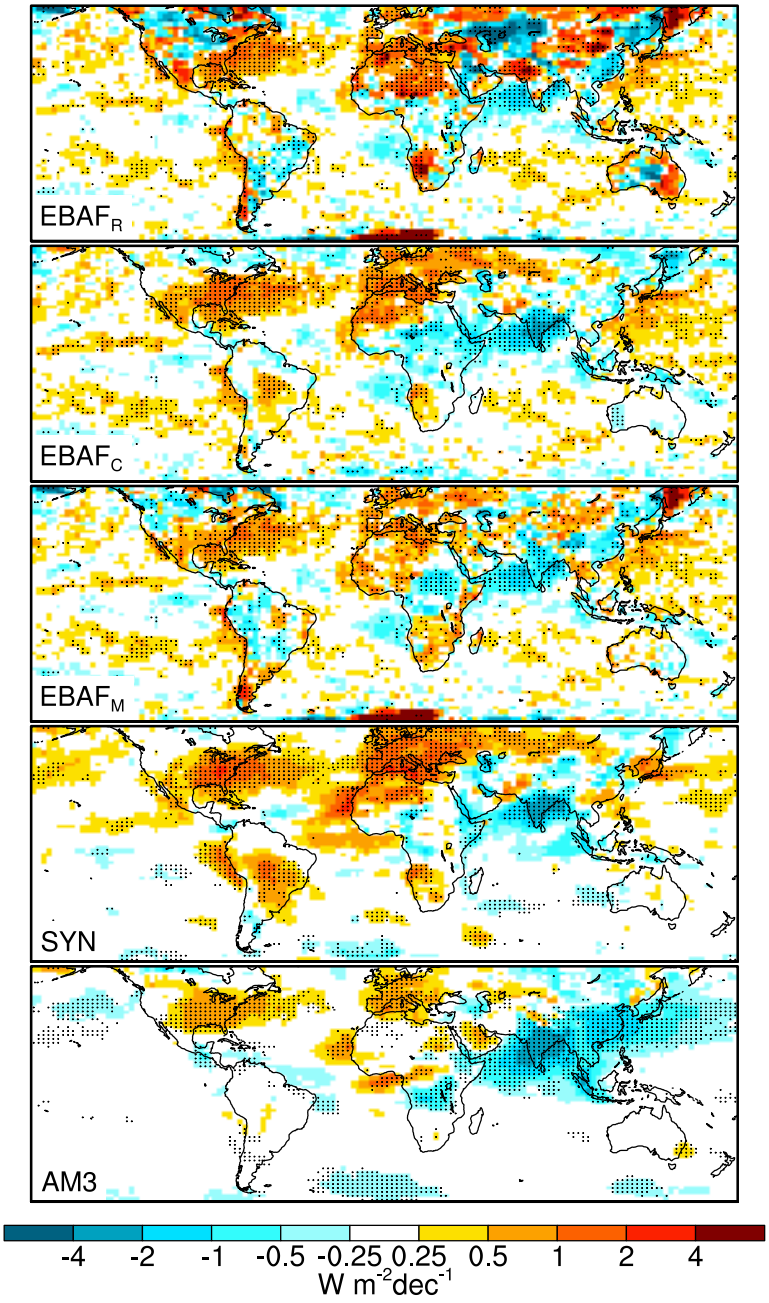


**Figure 2.** ~~Root mean square~~ Decadal rate of change in the ~~annual anomaly~~ clear-sky shortwave aerosol shortwave direct radiative effect ($DRE^{sw}_{clr}$). An increase in $DRE^{sw}_{clr}$ reflects a decrease in the amount of radiation scattered to space by aerosols. $EBAF_R$ is based on the outgoing clear-sky shortwave radiation ~~without~~ from CERES EBAF assuming its variability is solely associated with aerosols~~(Rsutcsaf)~~. $EBAF_C$ and ~~its decrease~~ $EBAF_M$ are estimated using the observed clear-sky outgoing shortwave fluxes from CERES EBAF after accounting for the ~~effect~~ variability of ~~albedo (B), albedo and~~ water vapor~~(C)~~, ~~albedo~~ozone, ~~water vapor, and ozone (D)~~surface albedo from CERES-EBAF and MODIS, ~~as described in equation ??~~respectively. ~~The area weighted RMS over land~~ Estimates from ~~60S to 60N in~~ ~~indicated in each panel~~SYN (calculation constrained by observations) and from the GFDL AM3 global chemistry-climate model are also shown. Dotted areas are significant at the 95% confidence level.

~~Decadal rate of change in the aerosol shortwave direct effect under clear sky (SDRECS). An increase in~~

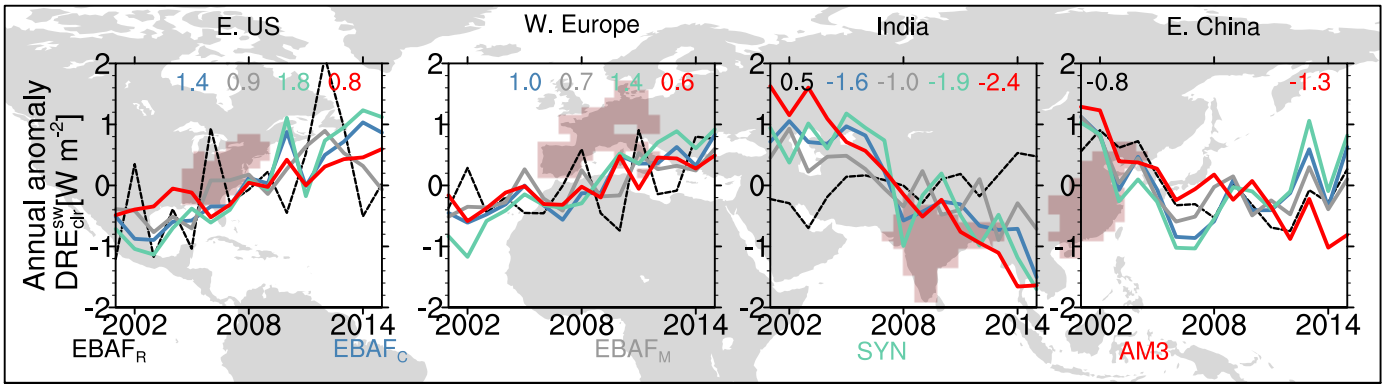


**Figure 3.** Regional changes in the ~~annual anomaly of the aerosol~~ clear-sky shortwave aerosol direct radiative effect ~~under clear sky (~~derived from ~~CERES-SYN~~ CERES-EBAF outgoing radiation without correction (~~SDRECS$_{CS}$,~~ EBAF$_R$ (black)) and after correcting for the variability of water, ozone, and surface albedo (from CERES-EBAF ~~corrected using CERES (SDRECS$_{CE}$~~EBAF$_C$, ~~grey~~blue) ~~, and~~ or from MODIS (~~SDRECS$_M$~~EBAF$_M$, grey)~~surface albedo~~) over the Eastern US, Western Europe, India, and Eastern China. ~~The simulated annual anomaly in SDRECS$_{AM3}$ and in the outgoing shortwave radiation Rsutes~~ Estimates from SYN (~~plotted as -Rsutes for consistency with the definition of SDRECS~~calculation constrained by observations) and from the GFDL AM3 global chemistry-climate model are shown in ~~red~~ green and ~~blue,~~ red respectively. The ~~magnitude~~ rate of ~~the linear decadal trend of~~ change for each ~~timeseries (in W m$^{-2}$ dec$^{-1}$)~~ estimate is indicated in ~~inset~~ W m$^{-2}$ dec$^{-1}$ when ~~the trend is~~ significant ~~at p=~~($p$<0.05).

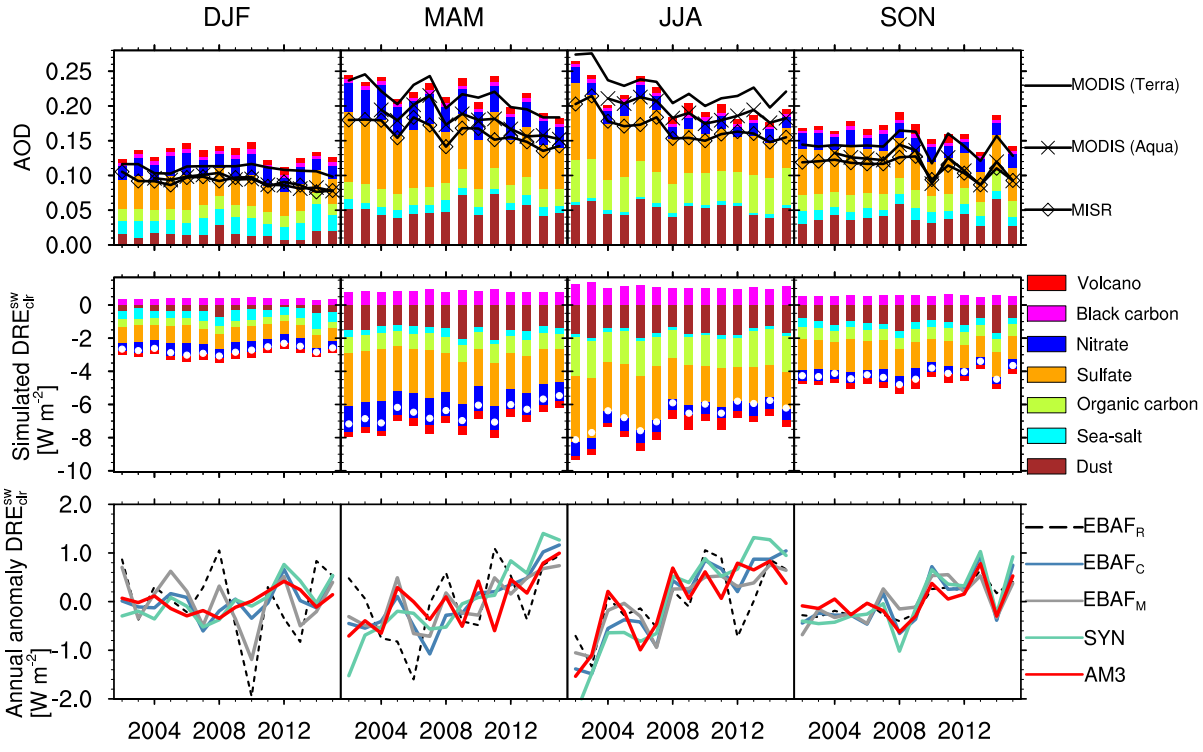


**Figure 4.** Seasonal changes in the aerosol optical depth (AOD) and ~~SDRECS~~ clear-sky shortwave aerosol direct radiative effect ($DRE^{sw}_{clr}$) in Western Europe (Fig. 3). The top row shows the ~~observed aerosol optical depth~~ AOD retrieved from different ~~space-borne platforms~~ spaceborne instruments (MODIS-Terra (lines), MODIS-Aqua (cross), MISR (diamond)) and the simulated ~~model~~ AOD decomposed into its components (bars). The second row shows the ~~individual~~ simulated clear-sky shortwave aerosol ~~SDRECS~~ direct radiative effect of individual aerosols (bars) and the ~~net SDRECS~~ overall aerosol direct radiative effect (white circle). The bottom ~~roTw~~ row shows ~~the observed~~ observation-based and simulated ~~seasonal anomalies~~ estimates of changes in ~~SDRECS (solid lines) and Rstucs (dash blue line)~~the aerosol direct radiative effect.

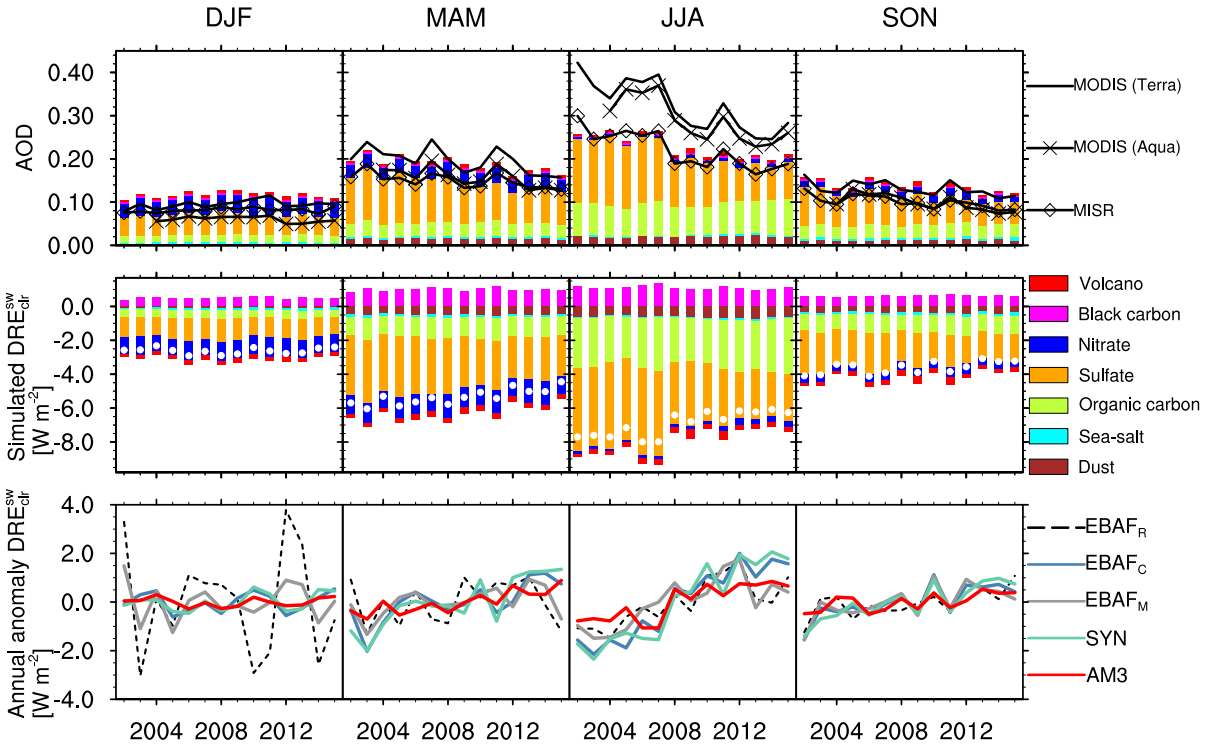


**Figure 5.** Same as 4 for the Eastern US

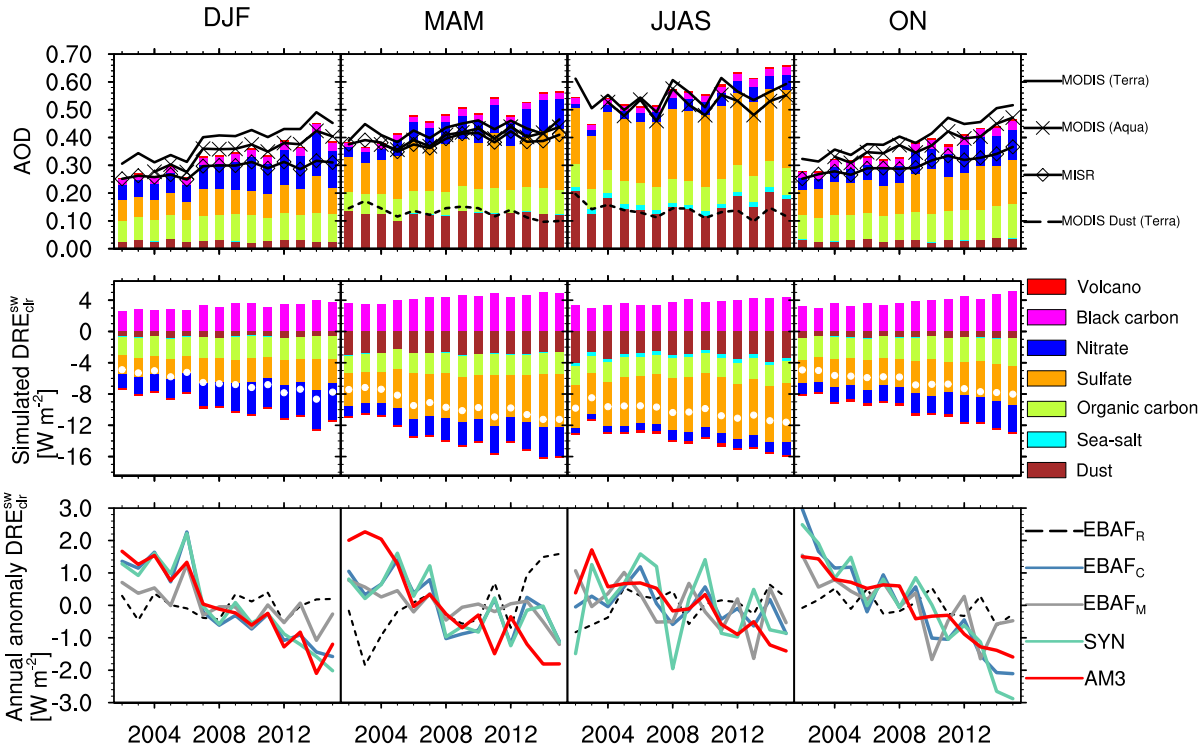


**Figure 6.** Same as 4 for the India. MISR is excluded in the monsoon season, when its coverage is too sparse relative to MODIS (TERRA). The MODIS-derived dust optical depth is indicated by a black dash line.

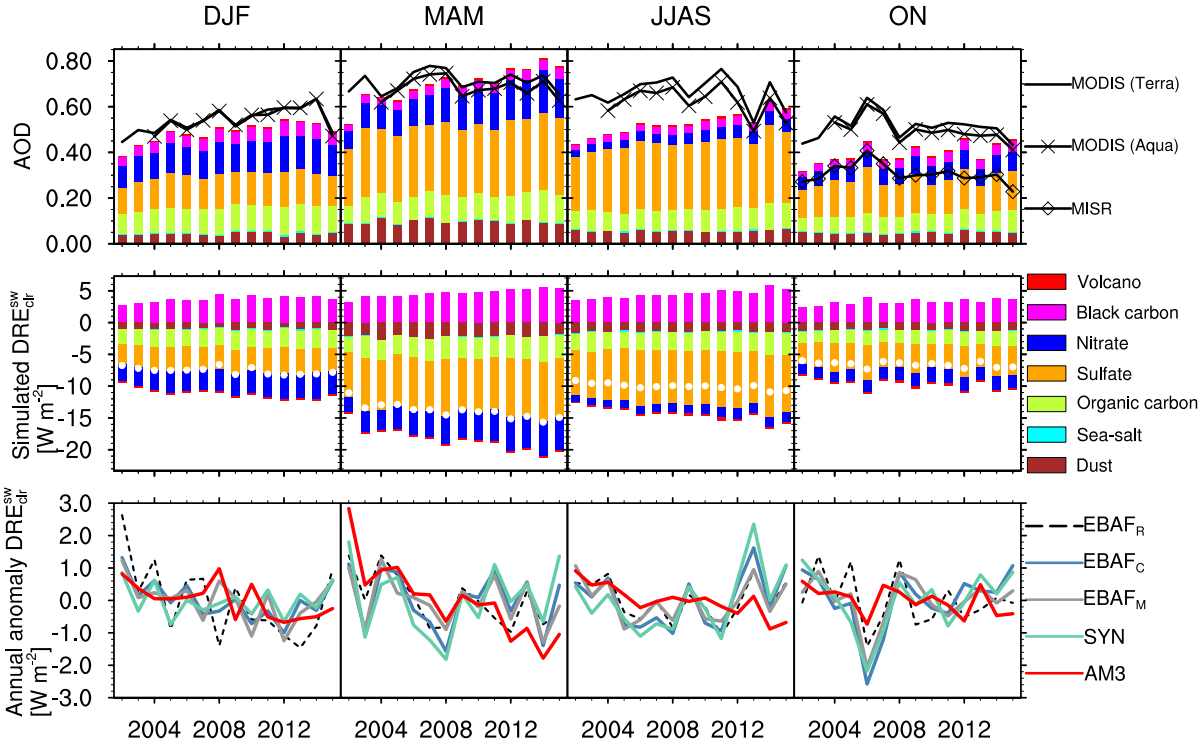


**Figure 7.** Same as 4 for Eastern China. MISR is excluded in winter, spring, and monsoon seasons, when its coverage is too sparse.

~~same as Fig. 7 but with MEIC $SO_2$ and NO emissions, revised $NH_3$ seasonality, and heterogeneous oxidation of $SO_2$ (see text)~~

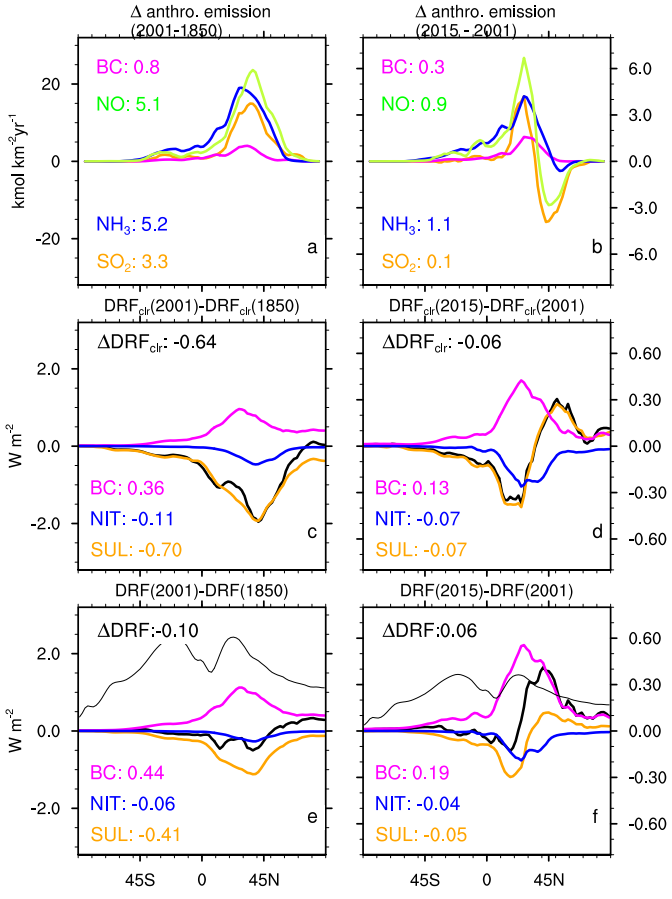


**Figure 8.** Meridional distribution of changes in anthropogenic emissions (BC, NO, $NH_3$, and $SO_2$) and in clear-sky (~~DRFCS~~$DRF_{clr}$, middle row) and all-sky radiative aerosol direct radiative forcing (DRF, bottom row) from 1850 to 2001 (left) and from 2001 to 2015 (right). The thin black line indicates the instantaneous radiative forcing at TOA from well-mixed greenhouse gases. Global anthropogenic emissions and the total and speciated ~~DRFCS~~ $DRF_{clr}$ and DRF are indicated inline.

**Table 1.** ~~Observation-based estimates and simulated decadal trends~~ Trends in the aerosol optical depth (AOD, ~~SDRECS~~ $\mathrm{dec}^{-1}$), and direct clear-sky shortwave radiative effect ($\mathrm{DRE}^{\mathrm{sw}}_{\mathrm{clr}}$, $\mathrm{W\,m^{-2}\,dec^{-1}}$) for selected regions and seasons from 2002 to 2015[a]

| | Western Europe | | Eastern US | | India | | Eastern China |
|---|---|---|---|---|---|---|---|
| | MAM | JJA | MAM | JJA | DJF | MAM | MAM |
| AOD | | | | | | | |
| MODIS (TERRA) | -0.04 [0.21] | -0.04 [0.23] | -0.04 [0.20] | -0.11 [0.32] | 0.13 [0.39] | 0.04 [0.43] | * [0.71] |
| MODIS (AQUA) | -0.05 [0.18] | -0.03 [0.19] | -0.04 [0.16] | -0.10 [0.29] | 0.11 [0.35] | 0.07 [0.40] | * [0.68] |
| MISR | -0.03 [0.16] | -0.03 [0.17] | -0.02 [0.15] | -0.08 [0.22] | 0.05 [0.29] | * [0.39] | |
| MATCH[b] | -0.06 [0.27] | -0.06 [0.26] | -0.07 [0.29] | -0.11 [0.35] | 0.03 [0.49] | * [0.64] | * [0.90] |
| AM3 | -0.04 [0.22] | -0.05 [0.21] | -0.03 [0.19] | -0.05 [0.23] | 0.13 [0.33] | 0.15 [0.47] | 0.15 [0.70] |
| sulfate | -0.03 [0.08] | -0.04 [0.07] | -0.03 [0.09] | -0.06 [0.12] | 0.02 [0.09] | 0.07 [0.17] | 0.05 [0.30] |
| nitrate | -0.01 [0.04] | * [0.02] | * [0.03] | 0.00 [0.01] | 0.07 [0.10] | 0.06 [0.07] | 0.08 [0.14] |
| black carbon | * [0.01] | * [0.00] | * [0.01] | * [0.00] | 0.01 [0.02] | 0.01 [0.02] | 0.01 [0.04] |
| $\mathrm{DRE}^{\mathrm{sw}}_{\mathrm{clr}}$ | | | | | | | |
| SYN | 1.8 [-8.9] | 2.5 [-9.4] | 2.1 [-8.6] | 3.6 [-11.0] | -2.6 [-9.1] | -1.4 [-13.4] | * [-20.5] |
| $\mathrm{EBAF_C}$ | 1.4 | 1.8 | 1.4 | 3.4 | -2.3 | -1.2 | * |
| $\mathrm{EBAF_M}$ | 1.0 | 1.2 | * | 2.0 | -0.8 | -0.9 | * |
| AM3 | 1.1 [-6.5] | 1.5 [-6.6] | 0.9 [-5.3] | 1.4 [-6.9] | -2.7 [-6.6] | -3.1 [-9.4] | -2.1 [-13.9] |
| sulfate | 0.9 [-2.6] | 1.5 [-2.7] | 1.1 [-3.1] | 2.2 [-3.9] | -0.7 [-2.9] | -1.8 [-5.5] | -1.1 [-8.5] |
| nitrate | 0.3 [-1.4] | * [-0.7] | * [-1.2] | -0.2 [-0.2] | -2.4 [-3.3] | -1.9 [-2.6] | -2.2 [-4.2] |
| black carbon | * [0.8] | -0.2 [1.1] | * [1.0] | * [1.1] | 0.9 [3.2] | 1.2 [4.3] | 1.4 [4.7] |

[a] The average over the period 2002–2015 is shown in bracket (2003-2015 for AQUA). Trends are estimated using the Theil-Sen method. * denotes non significant monotonous change at $p = 0.05$. Model AOD is sampled based on MODIS (TERRA) seasonal coverage. No statistics is provided for China from MISR because of large differences in spatial coverage with MODIS (TERRA). SYN refers to the aerosol effect caculated in the CERES-SYN product. $\mathrm{EBAF_C}$ and $\mathrm{EBAF_M}$ refer to the aerosol effect estimated using CERES-EBAF outgoing shortwave clear-sky radiation corrected for the variabily in water, ozone, and CERES-EBAF ($\mathrm{EBAF_C}$) and MODIS ($\mathrm{EBAF_M}$) surface albedo.

[b] from CERES-SYN Ed4 based on assimilation of MODIS Collection5 AOD with the MATCH model.

## References


Alfaro-Contreras, R., Zhang, J., Reid, J. S., and Christopher, S.: A Study of the Longer Term Variation of Aerosol Optical Thickness and Direct Shortwave Aerosol Radiative Effect Trends Using MODIS and CERES, Atmos. Chem. Phys. Discuss., 2017, 1–63, doi:10.5194/acp-2017-365, https://www.atmos-chem-phys-discuss.net/acp-2017-365/, 2017.

Ansari, A. S. and Pandis, S. N.: Response of Inorganic PM to Precursor Concentrations, Environ. Sci. Technol., 32, 2706–2714, 1998.

Babu, S. S., Manoj, M. R., Moorthy, K. K., Gogoi, M. M., Nair, V. S., Kompalli, S. K., Satheesh, S. K., Niranjan, K., Ramagopal, K., Bhuyan, P. K., and Singh, D.: Trends in aerosol optical depth over Indian region: Potential causes and impact indicators, Journal of Geophysical Research: Atmospheres, 118, 2013JD020 507, doi:10.1002/2013JD020507, http://onlinelibrary.wiley.com/doi/10.1002/2013JD020507/abstract, 2013.

Bellouin, N., Boucher, O., Haywood, J., and Reddy, M. S.: Global estimate of aerosol direct radiative forcing from satellite measurements, Nature, 438, 1138–1141, doi:10.1038/nature04348, https://doi.org/10.1038/nature04348, 2005.

Bellouin, N., Jones, A., Haywood, J., and Christopher, S. A.: Updated estimate of aerosol direct radiative forcing from satellite observations and comparison against the Hadley Centre climate model, Journal of Geophysical Research: Atmospheres, 113, n/a–n/a, doi:10.1029/2007JD009385, http://dx.doi.org/10.1029/2007JD009385, d10205, 2008.

Bollasina, M. A., Ming, Y., and Ramaswamy, V.: Anthropogenic Aerosols and the Weakening of the South Asian Summer Monsoon, Science, 334, 502–505, doi:10.1126/science.1204994, http://science.sciencemag.org/content/334/6055/502, 2011.

Bond, T. C., Doherty, S. J., Fahey, D. W., Forster, P. M., Berntsen, T., DeAngelo, B. J., Flanner, M. G., Ghan, S., Kärcher, B., Koch, D., Kinne, S., Kondo, Y., Quinn, P. K., Sarofim, M. C., Schultz, M. G., Schulz, M., Venkataraman, C., Zhang, H., Zhang, S., Bellouin, N., Guttikunda, S. K., Hopke, P. K., Jacobson, M. Z., Kaiser, J. W., Klimont, Z., Lohmann, U., Schwarz, J. P., Shindell, D., Storelvmo, T., Warren, S. G., and Zender, C. S.: Bounding the role of black carbon in the climate system: A scientific assessment, Journal of Geophysical Research: Atmospheres, 118, 5380–5552, doi:10.1002/jgrd.50171, http://dx.doi.org/10.1002/jgrd.50171, 2013.

Boucher, O., Randall, D., Artaxo, P., Bretherton, C., Feingold, G., Forster, P., Kerminen, V.-M., Kondo, Y., Liao, H., Lohmann, U., Rasch, P., Satheesh, S., Sherwood, S., Stevens, B., and Zhang, X.: Clouds and Aerosols, book section 7, pp. 571–658, Cambridge University Press, Cambridge, United Kingdom and New York, NY, USA, doi:10.1017/CBO9781107415324.016, www.climatechange2013.org, 2013.

CERES: CERES EBAF Ed4.0 Data Quality Summary, NASA, https://ceres.larc.nasa.gov/documents/DQ_summaries/CERES_EBAF_Ed4.0_DQS.pdf, 2017.

Cescatti, A., Marcolla, B., Santhana Vannan, S. K., Pan, J. Y., Román, M. O., Yang, X., Ciais, P., Cook, R. B., Law, B. E., Matteucci, G., Migliavacca, M., Moors, E., Richardson, A. D., Seufert, G., and Schaaf, C. B.: Intercomparison of MODIS albedo retrievals and in situ measurements across the global FLUXNET network, Remote Sens. Environ., 121, 323–334, doi:10.1016/j.rse.2012.02.019, http://www.sciencedirect.com/science/article/pii/S0034425712001125, 2012.

Charlson, R. J., Schwartz, S. E., Hales, J. M., Cess, R. D., Coakley, J. A., Hansen, J. E., and Hofmann, D. J.: Climate Forcing by Anthropogenic Aerosols, Science, 255, 423–430, doi:10.1126/science.255.5043.423, http://science.sciencemag.org/content/255/5043/423, 1992.

Cheng, Y., Zheng, G., Wei, C., Mu, Q., Zheng, B., Wang, Z., Gao, M., Zhang, Q., He, K., Carmichael, G., schl, U. P., and Su, H.: Reactive nitrogen chemistry in aerosol water as a source of sulfate during haze events in China, Sci. Adv., 2, e1601 530–e1601 530, doi:10.1126/sciadv.1601530, https://doi.org/10.1126/sciadv.1601530, 2016.

Christopher, S. A. and Zhang, J.: Cloud-free shortwave aerosol radiative effect over oceans: Strategies for identifying anthropogenic forcing from Terra satellite measurements, Geophys. Res. Lett., 31, n/a–n/a, doi:10.1029/2004GL020510, http://dx.doi.org/10.1029/2004GL020510, l18101, 2004.

Collins, W. D., Rasch, P. J., Eaton, B. E., Khattatov, B. V., Lamarque, J.-F., and Zender, C. S.: Simulating aerosols using a chemical transport model with assimilation of satellite aerosol retrievals: Methodology for INDOEX, Journal of Geophysical Research: Atmospheres, 106, 7313–7336, doi:10.1029/2000JD900507, http://onlinelibrary.wiley.com/doi/10.1029/2000JD900507/abstract, 2001.

de Foy, B., Lu, Z., and Streets, D. G.: Satellite NO2 retrievals suggest China has exceeded its NOx reduction goals from the twelfth Five-Year Plan, Sci. Rep., 6, doi:10.1038/srep35912, https://www.ncbi.nlm.nih.gov/pmc/articles/PMC5082360/, 2016.

Dentener, F., Kinne, S., Bond, T., Boucher, O., Cofala, J., Generoso, S., Ginoux, P., Gong, S., Hoelzemann, J. J., Ito, A., Marelli, L., Penner, J. E., Putaud, J.-P., Textor, C., Schulz, M., van der Werf, G. R., and Wilson, J.: Emissions of primary aerosol and precursor gases in the years 2000 and 1750 prescribed data-sets for AeroCom, Atmos. Chem. Phys., 6, 4321–4344, doi:10.5194/acp-6-4321-2006, https://doi.org/10.5194/acp-6-4321-2006, 2006.

Ding, J., Miyazaki, K., van der A, R. J., Mijling, B., Kurokawa, J.-I., Cho, S., Janssens-Maenhout, G., Zhang, Q., Liu, F., and Levelt, P. F.: Intercomparison of NOx emission inventories over East Asia, Atmos. Chem. Phys., 17, 10 125–10 141, doi:10.5194/acp-17-10125-2017, https://www.atmos-chem-phys.net/17/10125/2017/, 2017.

Donner, L. J., Wyman, B. L., Hemler, R. S., Horowitz, L. W., Ming, Y., Zhao, M., Golaz, J.-C., Ginoux, P., Lin, S.-J., Schwarzkopf, M. D., Austin, J., Alaka, G., Cooke, W. F., Delworth, T. L., Freidenreich, S. M., Gordon, C. T., Griffies, S. M., Held, I. M., Hurlin, W. J., Klein, S. A., Knutson, T. R., Langenhorst, A. R., Lee, H.-C., Lin, Y., Magi, B. I., Malyshev, S. L., Milly, P. C. D., Naik, V., Nath, M. J., Pincus, R., Ploshay, J. J., Ramaswamy, V., Seman, C. J., Shevliakova, E., Sirutis, J. J., Stern, W. F., Stouffer, R. J., Wilson, R. J., Winton, M., Wittenberg, A. T., and Zeng, F.: The Dynamical Core, Physical Parameterizations, and Basic Simulation Characteristics of the Atmospheric Component AM3 of the GFDL Global Coupled Model CM3, J. Clim., 24, 3484–3519, 2011.

Freidenreich, S. M. and Ramaswamy, V.: A new multiple-band solar radiative parameterization for general circulation models, Journal of Geophysical Research: Atmospheres, 104, 31 389–31 409, doi:10.1029/1999jd900456, https://doi.org/10.1029/1999jd900456, 1999.

Ginoux, P., Chin, M., Tegen, I., Prospero, J. M., Holben, B., Dubovik, O., and Lin, S.-J.: Sources and distributions of dust aerosols simulated with the GOCART model, J. Geophys. Res. Atmos., 106, 20 255–20 273, 2001.

Ginoux, P., Prospero, J. M., Gill, T. E., Hsu, N. C., and Zhao, M.: Global-scale attribution of anthropogenic and natural dust sources and their emission rates based on MODIS Deep Blue aerosol products, Rev. Geophys., 50, RG3005, 2012.

Griffies, S. M., Winton, M., Donner, L. J., Horowitz, L. W., Downes, S. M., Farneti, R., Gnanadesikan, A., Hurlin, W. J., Lee, H.-C., Liang, Z., Palter, J. B., Samuels, B. L., Wittenberg, A. T., Wyman, B. L., Yin, J., and Zadeh, N.: The GFDL CM3 Coupled Climate Model: Characteristics of the Ocean and Sea Ice Simulations, J. Clim., 24, 3520–3544, doi:10.1175/2011JCLI3964.1, http://journals.ametsoc.org/doi/abs/10.1175/2011JCLI3964.1, 2011.

Guenther, A., Karl, T., Harley, P., Wiedinmyer, C., Palmer, P. I., and Geron, C.: Estimates of global terrestrial isoprene emissions using MEGAN (Model of Emissions of Gases and Aerosols from Nature), Atmos. Chem. Phys., 6, 3181–3210, 2006.

Guo, H., Weber, R. J., and Nenes, A.: High levels of ammonia do not raise fine particle pH sufficiently to yield nitrogen oxide-dominated sulfate production, Sci. Rep., 7, doi:10.1038/s41598-017-11704-0, https://doi.org/10.1038/s41598-017-11704-0, 2017.

He, P., Alexander, B., Geng, L., Chi, X., Fan, S., Zhan, H., Kang, H., Zheng, G., Cheng, Y., Su, H., Liu, C., and Xie, Z.: Isotopic constraints on heterogeneous sulphate production in Beijing haze, Atmos. Chem. Phys. Discuss., pp. 1–25, doi:10.5194/acp-2017-977, https://doi.org/10.5194/acp-2017-977, 2017.

Heald, C. L., Collett, J. L., Lee, T., Benedict, K. B., Schwandner, F. M., Li, Y., Clarisse, L., Hurtmans, D. R., Van Damme, M., Clerbaux, C., Coheur, P.-F., and Pye, H. O. T.: Atmospheric ammonia and particulate inorganic nitrogen over the United States, Atmos. Chem. Phys., 12, 10 295–10 312, 2012.

Heald, C. L., Ridley, D. A., Kroll, J. H., Barrett, S. R. H., Cady-Pereira, K. E., Alvarado, M. J., and Holmes, C. D.: Contrasting the direct radiative effect and direct radiative forcing of aerosols, Atmos. Chem. Phys., 14, 5513–5527, doi:10.5194/acp-14-5513-2014, http://www.atmos-chem-phys.net/14/5513/2014/, 2014.

Hoesly, R. M., Smith, S. J., Feng, L., Klimont, Z., Janssens-Maenhout, G., Pitkanen, T., Seibert, J. J., Vu, L., Andres, R. J., Bolt, R. M., Bond, T. C., Dawidowski, L., Kholod, N., Kurokawa, J.-I., Li, M., Liu, L., Lu, Z., Moura, M. C. P., O'Rourke, . P. R., and Zhang, Q.: Historical (1750–2014) anthropogenic emissions of reactive gases and aerosols from the Community Emissions Data System (CEDS), Geosci. Model Dev., 11, 369–408, doi:10.5194/gmd-11-369-2018, https://www.geosci-model-dev.net/11/369/2018/, 2018.

Hung, H.-M. and Hoffmann, M. R.: Oxidation of gas-phase $SO_2$ on the surfaces of acidic microdroplets: implications for sulfate and sulfate radical anion formation in the atmospheric liquid phase, Environ. Sci. Technol., 49, 13 768–13 776, doi:10.1021/acs.est.5b01658, http://dx.doi.org/10.1021/acs.est.5b01658, 2015.

Irie, H., Muto, T., Itahashi, S., Kurokawa, J.-i., and Uno, I.: Turnaround of Tropospheric Nitrogen Dioxide Pollution Trends in China, Japan, and South Korea, Sola, 12, 170–174, doi:10.2151/sola.2016-035, 2016.

Jin, Q. and Wang, C.: The greening of Northwest Indian subcontinent and reduction of dust abundance resulting from Indian summer monsoon revival, Scientific Reports, 8, doi:10.1038/s41598-018-23055-5, https://doi.org/10.1038/s41598-018-23055-5, 2018.

John, J. G., Fiore, A. M., Naik, V., Horowitz, L. W., and Dunne, J. P.: Climate versus emission drivers of methane lifetime against loss by tropospheric OH from 1860–2100, Atmos. Chem. Phys., 12, 12 021–12 036, 2012.

Kahn, R. A.: Reducing the Uncertainties in Direct Aerosol Radiative Forcing, Surv. Geophys., 33, 701–721, doi:10.1007/s10712-011-9153-z, https://link.springer.com/article/10.1007/s10712-011-9153-z, 2012.

Kahn, R. A., Gaitley, B. J., Martonchik, J. V., Diner, D. J., Crean, K. A., and Holben, B.: Multiangle Imaging Spectroradiometer (MISR) global aerosol optical depth validation based on 2 years of coincident Aerosol Robotic Network (AERONET) observations, Journal of Geophysical Research: Atmospheres, 110, n/a–n/a, doi:10.1029/2004JD004706, http://dx.doi.org/10.1029/2004JD004706, d10S04, 2005.

Kahn, R. A., Gaitley, B. J., Garay, M. J., Diner, D. J., Eck, T. F., Smirnov, A., and Holben, B. N.: Multiangle Imaging SpectroRadiometer global aerosol product assessment by comparison with the Aerosol Robotic Network, Journal of Geophysical Research: Atmospheres, 115, n/a–n/a, doi:10.1029/2010JD014601, http://dx.doi.org/10.1029/2010JD014601, d23209, 2010.

Kalnay, E., Kanamitsu, M., Kistler, R., Collins, W., Deaven, D., Gandin, L., Iredell, M., Saha, S., White, G., Woollen, J., Zhu, Y., Leetmaa, A., Reynolds, R., Chelliah, M., Ebisuzaki, W., Higgins, W., Janowiak, J., Mo, K. C., Ropelewski, C., Wang, J., Jenne, R., and Joseph, D.: The NCEP/NCAR 40-Year Reanalysis Project, Bull. Am. Meteorol. Soc., 77, 437–471, 1996.

Kendall, M. G.: A new measure of rank correlation, Biometrika, 30, 81–93, doi:10.1093/biomet/30.1-2.81, +http://dx.doi.org/10.1093/biomet/30.1-2.81, 1938.

Kim, D., Chin, M., Bian, H., Tan, Q., Brown, M. E., Zheng, T., You, R., Diehl, T., Ginoux, P., and Kucsera, T.: The effect of the dynamic surface bareness on dust source function, emission, and distribution, Journal of Geophysical Research: Atmospheres, 118, 871–886, doi:10.1029/2012JD017907, http://onlinelibrary.wiley.com/doi/10.1029/2012JD017907/abstract, 2013.

Krotkov, N. A., McLinden, C. A., Li, C., Lamsal, L. N., Celarier, E. A., Marchenko, S. V., Swartz, W. H., Bucsela, E. J., Joiner, J., Duncan, B. N., Boersma, K. F., Veefkind, J. P., Levelt, P. F., Fioletov, V. E., Dickerson, R. R., He, H., Lu, Z., and Streets, D. G.: Aura OMI observations of regional SO2 and NO2 pollution changes from 2005 to 2015, Atmos. Chem. Phys., 16, 4605–4629, doi:10.5194/acp-16-4605-2016, https://www.atmos-chem-phys.net/16/4605/2016/, 2016.

Kühn, T., Partanen, A.-I., Laakso, A., Lu, Z., Bergman, T., Mikkonen, S., Kokkola, H., Korhonen, H., Räisänen, P., Streets, D. G., Romakkaniemi, S., and Laaksonen, A.: Climate impacts of changing aerosol emissions since 1996, Geophys. Res. Lett., 41, 4711–4718, doi:10.1002/2014gl060349, https://doi.org/10.1002/2014gl060349, 2014.

Levy, H., Horowitz, L. W., Schwarzkopf, M. D., Ming, Y., Golaz, J.-C., Naik, V., and Ramaswamy, V.: The roles of aerosol direct and indirect effects in past and future climate change, J. Geophys. Res. Atmos., 118, 4521–4532, 2013a.

Levy, R. C., Mattoo, S., Munchak, L. A., Remer, L. A., Sayer, A. M., Patadia, F., and Hsu, N. C.: The Collection 6 MODIS aerosol products over land and ocean, Atmos. Meas. Tech., 6, 2989–3034, doi:10.5194/amt-6-2989-2013, https://doi.org/10.5194/amt-6-2989-2013, 2013b.

Li, C., Zhang, Q., Krotkov, N. A., Streets, D. G., He, K., Tsay, S.-C., and Gleason, J. F.: Recent large reduction in sulfur dioxide emissions from Chinese power plants observed by the Ozone Monitoring Instrument, Geophys. Res. Lett., 37, n/a–n/a, doi:10.1029/2010GL042594, http://dx.doi.org/10.1029/2010GL042594, l08807, 2010.

Liu, F., Zhang, Q., A, R. J. v. d., Zheng, B., Tong, D., Yan, L., Zheng, Y., and He, K.: Recent reduction in NO x emissions over China: synthesis of satellite observations and emission inventories, Environ. Res. Lett., 11, 114 002, doi:10.1088/1748-9326/11/11/114002, http://stacks.iop.org/1748-9326/11/i=11/a=114002, 2016.

Liu, J., Fan, S., Horowitz, L. W., and Levy, H.: Evaluation of factors controlling long-range transport of black carbon to the Arctic, J. Geophys. Res. Atmos., 116, D04 307, 2011.

Loeb, N. G. and Manalo-Smith, N.: Top-of-Atmosphere Direct Radiative Effect of Aerosols over Global Oceans from Merged CERES and MODIS Observations, J. Climate, 18, 3506–3526, doi:10.1175/JCLI3504.1, http://journals.ametsoc.org/doi/abs/10.1175/JCLI3504.1, 2005.

Loeb, N. G., Wielicki, B. A., Doelling, D. R., Smith, G. L., Keyes, D. F., Kato, S., Manalo-Smith, N., and Wong, T.: Toward Optimal Closure of the Earth's Top-of-Atmosphere Radiation Budget, J. Climate, 22, 748–766, doi:10.1175/2008JCLI2637.1, http://journals.ametsoc.org/doi/abs/10.1175/2008JCLI2637.1, 2009.

Loeb, N. G., Doelling, D. R., Wang, H., Su, W., Nguyen, C., Corbett, J. G., Liang, L., Mitrescu, C., Rose, F. G., and Kato, S.: Clouds and the Earth's Radiant Energy System (CERES) Energy Balanced and Filled (EBAF) Top-of-Atmosphere (TOA) Edition-4.0 Data Product, Journal of Climate, 31, 895–918, doi:10.1175/jcli-d-17-0208.1, https://doi.org/10.1175/jcli-d-17-0208.1, 2018.

Murphy, D. M.: Little net clear-sky radiative forcing from recent regional redistribution of aerosols, Nat. Geosci., 6, 258–262, doi:10.1038/ngeo1740, https://doi.org/10.1038/ngeo1740, 2013.

Myhre, G., Samset, B. H., Schulz, M., Balkanski, Y., Bauer, S., Berntsen, T. K., Bian, H., Bellouin, N., Chin, M., Diehl, T., Easter, R. C., Feichter, J., Ghan, S. J., Hauglustaine, D., Iversen, T., Kinne, S., Kirkevåg, A., Lamarque, J.-F., Lin, G., Liu, X., Lund, M. T., Luo, G., Ma, X., van Noije, T., Penner, J. E., Rasch, P. J., Ruiz, A., Seland, Ø., Skeie, R. B., Stier, P., Takemura, T., Tsigaridis, K., Wang, P., Wang, Z., Xu, L., Yu, H., Yu, F., Yoon, J.-H., Zhang, K., Zhang, H., and Zhou, C.: Radiative forcing of the direct aerosol effect from AeroCom Phase II simulations, Atmos. Chem. Phys., 13, 1853–1877, 2013.

Myhre, G., Aas, W., Cherian, R., Collins, W., Faluvegi, G., Flanner, M., Forster, P., Hodnebrog, Ø., Klimont, Z., Lund, M. T., Mülmenstädt, J., Lund Myhre, C., Olivié, D., Prather, M., Quaas, J., Samset, B. H., Schnell, J. L., Schulz, M., Shindell, D., Skeie, R. B., Takemura, T., and Tsyro, S.: Multi-model simulations of aerosol and ozone radiative forcing due to anthropogenic emission changes during the period 1990–2015, Atmospheric Chemistry and Physics, 17, 2709–2720, doi:10.5194/acp-17-2709-2017, https://www.atmos-chem-phys.net/17/2709/2017/, 2017.

Naik, V., Horowitz, L. W., Fiore, A. M., Ginoux, P., Mao, J., Aghedo, A. M., and Levy, H.: Impact of preindustrial to present-day changes in short-lived pollutant emissions on atmospheric composition and climate forcing, J. Geophys. Res. Atmos., 118, 8086–8110, 2013.

Oleson, K. W., Bonan, G. B., Schaaf, C., Gao, F., Jin, Y., and Strahler, A.: Assessment of global climate model land surface albedo using MODIS data, Geophys. Res. Lett., 30, n/a–n/a, doi:10.1029/2002GL016749, http://dx.doi.org/10.1029/2002GL016749, 1443, 2003.

Pan, X., Chin, M., Gautam, R., Bian, H., Kim, D., Colarco, P. R., Diehl, T. L., Takemura, T., Pozzoli, L., Tsigaridis, K., Bauer, S., and Bellouin, N.: A multi-model evaluation of aerosols over South Asia: common problems and possible causes, Atmos. Chem. Phys., 15, 5903–5928, doi:10.5194/acp-15-5903-2015, https://www.atmos-chem-phys.net/15/5903/2015/, 2015.

Patadia, F., Gupta, P., and Christopher, S. A.: First observational estimates of global clear sky shortwave aerosol direct radiative effect over land, Geophys. Res. Lett., 35, L04 810, doi:10.1029/2007GL032314, http://onlinelibrary.wiley.com/doi/10.1029/2007GL032314/abstract, 2008.

Paulot, F., Jacob, D. J., Pinder, R. W., Bash, J. O., Travis, K., and Henze, D. K.: Ammonia emissions in the United States, European Union, and China derived by high-resolution inversion of ammonium wet deposition data: Interpretation with a new agricultural emissions inventory (MASAGE_NH3), J. Geophys. Res. Atmos., 119, 4343–4364, 2014.

Paulot, F., Ginoux, P., Cooke, W. F., Donner, L. J., Fan, S., Lin, M.-Y., Mao, J., Naik, V., and Horowitz, L. W.: Sensitivity of nitrate aerosols to ammonia emissions and to nitrate chemistry: implications for present and future nitrate optical depth, Atmos. Chem. Phys., 16, 1459–1477, doi:10.5194/acp-16-1459-2016, http://www.atmos-chem-phys.net/16/1459/2016/, 2016.

Paulot, F., Fan, S., and Horowitz, L. W.: Contrasting seasonal responses of sulfate aerosols to declining $SO_2$ emissions in the Eastern U.S.: Implications for the efficacy of $SO_2$ emission controls, Geophys. Res. Lett., 44, 455–464, doi:10.1002/2016GL070695, http://dx.doi.org/10.1002/2016GL070695, 2016GL070695, 2017a.

Paulot, F., Paynter, D., Ginoux, P., Naik, V., Whitburn, S., Van Damme, M., Clarisse, L., Coheur, P.-F., and Horowitz, L. W.: Gas-aerosol partitioning of ammonia in biomass burning plumes: Implications for the interpretation of spaceborne observations of ammonia and the radiative forcing of ammonium nitrate, Geophys. Res. Lett., 44, 2017GL074 215, doi:10.1002/2017GL074215, http://onlinelibrary.wiley.com/doi/10.1002/2017GL074215/abstract, 2017b.

Rayner, N. A., Parker, D. E., Horton, E. B., Folland, C. K., Alexander, L. V., Rowell, D. P., Kent, E. C., and Kaplan, A.: Global analyses of sea surface temperature, sea ice, and night marine air temperature since the late nineteenth century, J. Geophys. Res. Atmos., 108, 4407, doi:10.1029/2002JD002670, http://dx.doi.org/10.1029/2002JD002670, 2003.

Rosenfeld, D., Andreae, M. O., Asmi, A., Chin, M., de Leeuw, G., Donovan, D. P., Kahn, R., Kinne, S., Kivekäs, N., Kulmala, M., Lau, W., Schmidt, K. S., Suni, T., Wagner, T., Wild, M., and Quaas, J.: Global observations of aerosol-cloud-precipitation-climate interactions, Rev. Geophys., 52, 2013RG000 441, doi:10.1002/2013RG000441, http://onlinelibrary.wiley.com/doi/10.1002/2013RG000441/abstract, 2014.

Rutan, D., Rose, F., Roman, M., Manalo-Smith, N., Schaaf, C., and Charlock, T.: Development and assessment of broadband surface albedo from Clouds and the Earth's Radiant Energy System Clouds and Radiation Swath data product, Journal of Geophysical Research: Atmospheres, 114, D08 125, doi:10.1029/2008JD010669, http://onlinelibrary.wiley.com/doi/10.1029/2008JD010669/abstract, 2009.

Rutan, D. A., Kato, S., Doelling, D. R., Rose, F. G., Nguyen, L. T., Caldwell, T. E., and Loeb, N. G.: CERES Synoptic Product: Methodology and Validation of Surface Radiant Flux, J. Atmos. Oceanic Technol., 32, 1121–1143, doi:10.1175/JTECH-D-14-00165.1, http://journals.ametsoc.org/doi/abs/10.1175/JTECH-D-14-00165.1, 2015.

Saikawa, E., Kim, H., Zhong, M., Avramov, A., Zhao, Y., Janssens-Maenhout, G., ichi Kurokawa, J., Klimont, Z., Wagner, F., Naik, V., Horowitz, L. W., and Zhang, Q.: Comparison of emissions inventories of anthropogenic air pollutants and greenhouse gases in China, Atmospheric Chemistry and Physics, 17, 6393–6421, doi:10.5194/acp-17-6393-2017, https://doi.org/10.5194/acp-17-6393-2017, 2017a.

Saikawa, E., Trail, M., Zhong, M., Wu, Q., Young, C. L., Janssens-Maenhout, G., Klimont, Z., Wagner, F., ichi Kurokawa, J., Nagpure, A. S., and Gurjar, B. R.: Uncertainties in emissions estimates of greenhouse gases and air pollutants in India and their impacts on regional air quality, Environmental Research Letters, 12, 065 002, doi:10.1088/1748-9326/aa6cb4, https://doi.org/10.1088/1748-9326/aa6cb4, 2017b.

Sayer, A. M., Munchak, L. A., Hsu, N. C., Levy, R. C., Bettenhausen, C., and Jeong, M.-J.: MODIS Collection 6 aerosol products: Comparison between Aqua's e-Deep Blue, Dark Target, and "merged" data sets, and usage recommendations, Journal of Geophysical Research: Atmospheres, 119, 13,965–13,989, doi:10.1002/2014JD022453, http://dx.doi.org/10.1002/2014JD022453, 2014JD022453, 2014.

Schaaf, C. B., Gao, F., Strahler, A. H., Lucht, W., Li, X., Tsang, T., Strugnell, N. C., Zhang, X., Jin, Y., Muller, J.-P., Lewis, P., Barnsley, M., Hobson, P., Disney, M., Roberts, G., Dunderdale, M., Doll, C., d'Entremont, R. P., Hu, B., Liang, S., Privette, J. L., and Roy, D.: First operational BRDF, albedo nadir reflectance products from MODIS, Remote Sens. Environ., 83, 135–148, doi:10.1016/S0034-4257(02)00091-3, http://www.sciencedirect.com/science/article/pii/S0034425702000913, 2002.

Schwarzkopf, M. D. and Ramaswamy, V.: Radiative effects of CH4, N2O, halocarbons and the foreign-broadened H2O continuum: A GCM experiment, Journal of Geophysical Research: Atmospheres, 104, 9467–9488, doi:10.1029/1999jd900003, https://doi.org/10.1029/1999jd900003, 1999.

Sen, P. K.: Estimates of the Regression Coefficient Based on Kendall's Tau, J. Am. Stat. Assoc., 63, 1379–1389, doi:10.1080/01621459.1968.10480934, http://www.tandfonline.com/doi/abs/10.1080/01621459.1968.10480934, 1968.

Stevens, B.: Rethinking the Lower Bound on Aerosol Radiative Forcing, J. Climate, 28, 4794–4819, doi:10.1175/JCLI-D-14-00656.1, https://doi.org/10.1175/JCLI-D-14-00656.1, 2015.

Stevens, B. and Schwartz, S. E.: Observing and Modeling Earth's Energy Flows, Surv. Geophys., 33, 779–816, doi:10.1007/s10712-012-9184-0, https://doi.org/10.1007/s10712-012-9184-0, 2012.

Stevens, B., Fiedler, S., Kinne, S., Peters, K., Rast, S., Müsse, J., Smith, S. J., and Mauritsen, T.: MACv2-SP: a parameterization of anthropogenic aerosol optical properties and an associated Twomey effect for use in CMIP6, Geosci. Model Dev., 10, 433–452, doi:10.5194/gmd-10-433-2017, https://www.geosci-model-dev.net/10/433/2017/, 2017.

Storelvmo, T., Leirvik, T., Lohmann, U., Phillips, P. C. B., and Wild, M.: Disentangling greenhouse warming and aerosol cooling to reveal Earth's climate sensitivity, Nat. Geosci., 9, 286–289, doi:10.1038/ngeo2670, http://www.nature.com/ngeo/journal/v9/n4/full/ngeo2670.html?foxtrotcallback=true, 2016.

Su, W., Loeb, N. G., Schuster, G. L., Chin, M., and Rose, F. G.: Global all-sky shortwave direct radiative forcing of anthropogenic aerosols from combined satellite observations and GOCART simulations, Journal of Geophysical Research: Atmospheres, 118, 655–669, doi:10.1029/2012jd018294, https://doi.org/10.1029/2012jd018294, 2013.

Tao, M., Chen, L., Wang, Z., Tao, J., Che, H., Wang, X., and Wang, Y.: Comparison and evaluation of the MODIS Collection 6 aerosol data in China, Journal of Geophysical Research: Atmospheres, 120, 6992–7005, doi:10.1002/2015jd023360, https://doi.org/10.1002/2015jd023360, 2015.

Taylor, K. E., Williamson, D., and Zwiers, F.: The sea surface temperature and sea-ice concentration boundary conditions for AMIP II simulations, Program for Climate Model Diagnosis and Intercomparison, Lawrence Livermore National Laboratory, University of California, 2000.

Theil, H.: A rank-invariant method of linear and polynomial regression analysis. I, Nederl. Akad. Wetensch., Proc., 53, 386–392 = Indagationes Math. 12, 85–91 (1950), http://www.ams.org/mathscinet-getitem?mr=0036489, 1950.

Twomey, S.: Pollution and the planetary albedo, Atmos. Environ., 8, 1251–1256, doi:10.1016/0004-6981(74)90004-3, http://www.sciencedirect.com/science/article/pii/0004698174900043, 1974.

van der A, R. J., Mijling, B., Ding, J., Koukouli, M. E., Liu, F., Li, Q., Mao, H., and Theys, N.: Cleaning up the air: effectiveness of air quality policy for $SO_2$ and $NO_x$ emissions in China, Atmos. Chem. Phys., 17, 1775–1789, doi:10.5194/acp-17-1775-2017, https://www.atmos-chem-phys.net/17/1775/2017/, 2017.

van der Werf, G. R., Randerson, J. T., Giglio, L., van Leeuwen, T. T., Chen, Y., Roğers, B. M., Mu, M., van Marle, M. J. E., Morton, D. C., Collatz, G. J., Yokelson, R. J., and Ķasibhatla, P. S.: Global fire emissions estimates during 1997–2016, Earth System Science Data, 9, 697–720, doi:10.5194/essd-9-697-2017, https://www.earth-syst-sci-data.net/9/697/2017/, 2017.

van Marle, M. J. E., Kloster, S., Magi, B. I., Marlon, J. R., Daniau, A.-L., Field, R. D., Arneth, A., Forrest, M., Hantson, S., Kehrwald, N. M., Knorr, W., Lasslop, G., Li, F., Mangeon, S., Yue, C., Kaiser, J. W., and van der Werf, G. R.: Historic global biomass burning emissions for CMIP6 (BB4CMIP) based on merging satellite observations with proxies and fire models (1750–2015), Geosci. Model Dev., 10, 3329–3357, doi:10.5194/gmd-10-3329-2017, https://doi.org/10.5194/gmd-10-3329-2017, 2017.

Vermote, E. F. and Kotchenova, S.: Atmospheric correction for the monitoring of land surfaces, Journal of Geophysical Research: Atmospheres, 113, D23S90, doi:10.1029/2007JD009662, http://onlinelibrary.wiley.com/doi/10.1029/2007JD009662/abstract, 2008.

Vermote, E. F. and Saleous, N.: Operational Atmospheric Correction of MODIS Visible to Middle Infrared Land Surface Data in the Case of an Infinite Lambertian Target, in: Earth Science Satellite Remote Sensing, pp. 123–153, Springer, Berlin, Heidelberg, https://link.springer.com/chapter/10.1007/978-3-540-37293-6_8, dOI: 10.1007/978-3-540-37293-6_8, 2006.

Vermote, E. F., El Saleous, N., Justice, C. O., Kaufman, Y. J., Privette, J. L., Remer, L., Roger, J. C., and Tanré, D.: Atmospheric correction of visible to middle-infrared EOS-MODIS data over land surfaces: Background, operational algorithm and validation, Journal of Geophysical Research: Atmospheres, 102, 17 131–17 141, doi:10.1029/97JD00201, http://onlinelibrary.wiley.com/doi/10.1029/97JD00201/abstract, 1997.

Vermote, E. F., El Saleous, N. Z., and Justice, C. O.: Atmospheric correction of MODIS data in the visible to middle infrared: first results, Remote Sens. Environ., 83, 97–111, doi:10.1016/S0034-4257(02)00089-5, http://www.sciencedirect.com/science/article/pii/S0034425702000895, 2002.

Wang, S., Xing, J., Jang, C., Zhu, Y., Fu, J. S., and Hao, J.: Impact Assessment of Ammonia Emissions on Inorganic Aerosols in East China Using Response Surface Modeling Technique, Environ. Sci. Technol., 45, 9293–9300, doi:10.1021/es2022347, http://dx.doi.org/10.1021/es2022347, 2011.

Wang, Y., Zhang, Q., Jiang, J., Zhou, W., Wang, B., He, K., Duan, F., Zhang, Q., Philip, S., and Xie, Y.: Enhanced sulfate formation during China's severe winter haze episode in January 2013 missing from current models, J. Geophys. Res. Atmos., 119, 2013JD021 426, doi:10.1002/2013JD021426, http://onlinelibrary.wiley.com/doi/10.1002/2013JD021426/abstract, 2014a.

Wang, Z., Schaaf, C. B., Strahler, A. H., Chopping, M. J., Román, M. O., Shuai, Y., Woodcock, C. E., Hollinger, D. Y., and Fitzjarrald, D. R.: Evaluation of MODIS albedo product (MCD43A) over grassland, agriculture and forest surface types during dormant and snow-covered periods, Remote Sens. Environ., 140, 60–77, doi:10.1016/j.rse.2013.08.025, http://www.sciencedirect.com/science/article/pii/S0034425713002836, 2014b.

Warner, J. X., Dickerson, R. R., Wei, Z., Strow, L. L., Wang, Y., and Liang, Q.: Increased atmospheric ammonia over the world's major agricultural areas detected from space, Geophys. Res. Lett., p. 2016GL072305, doi:10.1002/2016GL072305, http://onlinelibrary.wiley.com/doi/10.1002/2016GL072305/abstract, 2017.

Wielicki, B. A., Barkstrom, B. R., Harrison, E. F., Lee, R. B., Louis Smith, G., and Cooper, J. E.: Clouds and the Earth's Radiant Energy System (CERES): An Earth Observing System Experiment, Bull. Amer. Meteor. Soc., 77, 853–868, doi:10.1175/1520-0477(1996)077<0853:CATERE>2.0.CO;2, http://journals.ametsoc.org/doi/abs/10.1175/1520-0477(1996)077%3C0853%3ACATERE%3E2.0.CO%3B2, 1996.

Wielicki, B. A., Barkstrom, B. R., Baum, B. A., Charlock, T. P., Green, R. N., Kratz, D. P., Lee, R. B., Minnis, P., Smith, G. L., Wong, T., Young, D. F., Cess, R. D., Coakley, J. A., Crommelynck, D. A. H., Donner, L., Kandel, R., King, M. D., Miller, A. J., Ramanathan, V., Randall, D. A., Stowe, L. L., and Welch, R. M.: Clouds and the Earth's Radiant Energy System (CERES): algorithm overview, IEEE Trans. Geosci. Remote Sens., 36, 1127–1141, doi:10.1109/36.701020, 1998.

Wild, M.: Global dimming and brightening: A review, Journal of Geophysical Research: Atmospheres, 114, D00D16, doi:10.1029/2008JD011470, http://onlinelibrary.wiley.com/doi/10.1029/2008JD011470/abstract, 2009.

Wu, Y., de Graaf, M., and Menenti, M.: Improved MODIS Dark Target aerosol optical depth algorithm over land: angular effect correction, Atmos. Meas. Tech., 9, 5575–5589, doi:10.5194/amt-9-5575-2016, https://doi.org/10.5194/amt-9-5575-2016, 2016.

Xiao, Q., Zhang, H., Choi, M., Li, S., Kondragunta, S., Kim, J., Holben, B., Levy, R. C., and Liu, Y.: Evaluation of VIIRS,GOCI, and MODIS Collection 6 AOD retrievals against ground sunphotometer observations over East Asia, Atmos. Chem. Phys., 16, 1255–1269, doi:10.5194/acp-16-1255-2016, https://doi.org/10.5194/acp-16-1255-2016, 2016.

Xing, J., Mathur, R., Pleim, J., Hogrefe, C., Gan, C.-M., Wong, D. C., and Wei, C.: Can a coupled meteorology–chemistry model reproduce the historical trend in aerosol direct radiative effects over the Northern Hemisphere?, Atmos. Chem. Phys., 15, 9997–10 018, doi:10.5194/acp-15-9997-2015, https://www.atmos-chem-phys.net/15/9997/2015/, 2015.

Yevich, R. and Logan, J.: An assessment of biofuel use and burning of agricultural waste in the developing world., Global Biogeochem. Cycles, 17, 1095, 2003.

Zhang, L., Chen, Y., Zhao, Y., Henze, D. K., Zhu, L., Song, Y., Paulot, F., Liu, X., Pan, Y., and Huang, B.: Agricultural ammonia emissions in China: reconciling bottom-up and top-down estimates, Atmos. Chem. Phys. Discuss., 2017, 1–36, doi:10.5194/acp-2017-749, https://www.atmos-chem-phys-discuss.net/acp-2017-749/, 2017.

Zhang, Q., Streets, D. G., Carmichael, G. R., He, K. B., Huo, H., Kannari, A., Klimont, Z., Park, I. S., Reddy, S., Fu, J. S., Chen, D., Duan, L., Lei, Y., Wang, L. T., and Yao, Z. L.: Asian emissions in 2006 for the NASA INTEX-B mission, Atmos. Chem. Phys., 9, 5131–5153, doi:10.5194/acp-9-5131-2009, https://www.atmos-chem-phys.net/9/5131/2009/, 2009.

Zhao, B., Jiang, J. H., Gu, Y., Diner, D., Worden, J., Liou, K.-N., Su, H., Xing, J., Michael Garay, and Huang, L.: Decadal-scale trends in regional aerosol particle properties and their linkage to emission changes, Environ. Res. Lett., 12, 054 021, doi:10.1088/1748-9326/aa6cb2, http://stacks.iop.org/1748-9326/12/i=5/a=054021, 2017.

Zheng, B., Zhang, Q., Zhang, Y., He, K. B., Wang, K., Zheng, G. J., Duan, F. K., Ma, Y. L., and Kimoto, T.: Heterogeneous chemistry: a mechanism missing in current models to explain secondary inorganic aerosol formation during the January 2013 haze episode in North China, Atmos. Chem. Phys., 15, 2031–2049, doi:10.5194/acp-15-2031-2015, http://www.atmos-chem-phys.net/15/2031/2015/, 2015.

Zhu, Z., Piao, S., Myneni, R. B., Huang, M., Zeng, Z., Canadell, J. G., Ciais, P., Sitch, S., Friedlingstein, P., Arneth, A., Cao, C., Cheng, L., Kato, E., Koven, C., Li, Y., Lian, X., Liu, Y., Liu, R., Mao, J., Pan, Y., Peng, S., Peñuelas, J., Poulter, B., Pugh, T. A. M., Stocker, B. D., Viovy, N., Wang, X., Wang, Y., Xiao, Z., Yang, H., Zaehle, S., and Zeng, N.: Greening of the Earth and its drivers, Nature Climate Change, 6, 791–795, doi:10.1038/nclimate3004, https://doi.org/10.1038/nclimate3004, 2016.